ISSN No. 2277-7628

Journal of Modern Science

Vol.7 - No.2 Price : ₹ 50/- November 2015

1. Antibacterial Activity of Marine Microalgae from Enayam Coast, West Coast of India 1
2. Computing Median with Data Depth in Multivariate Data 11
3. Effect of organic manure in controlling environmental pollution 20
4. Solar assisted photocatalytic degradation of reactive organge 4 to mineral acid by fluorinated TiO_2 wackherr 27
5. A High-Availability and Integrity of Data for Cloud Storage in Cloud Computing 43
6. MHD boundary layer flow of Nanofluid past an infinite vertical plate with chemical reaction, heat source, radiation and ohmic dissipation effects 56

Tamil Nadu State Council for Higher Education

Chennai - 600 005

Annual Subscription : Individuals ₹ 90/-
Institutions ₹ 150/-

Half - Yearly

TAMIL NADU STATE COUNCIL FOR HIGHER EDUCATION, CHENNAI-5

Vol. 7 November 2015

No. 2 Price : ₹ 50/-

ISSN 2277 - 7628

JOURNAL OF MODERN SCIENCE

A Half Yearly Journal of Higher Education published by
Tamil Nadu State Council for Higher Education

ARTICLES

1. Antibacterial Activity of Marine Microalgae from Enayam Coast, West Coast of India 1

2. Computing Median with Data Depth in Multivariate Data 11

3. Effect of organic manure in controlling environmental pollution 20

4. Solar assisted photocatalytic degradation of reactive organge 4 to mineral acid by fluorinated TiO_2 wackherr 27

5. A High-Availability and Integrity of Data for Cloud Storage in Cloud Computing 43

6. MHD boundary layer flow of Nanofluid past an infinite vertical plate with chemical reaction, heat source, radiation and ohmic dissipation effects 56

GUIDELINES FOR SUBMISSION OF MANUSCRIPTS

1. Manuscripts should be submitted in duplicate. It must be typed on one side only, double-spaced, with sufficient margins on all sides to facilitate editing and styling.
2. Charts, tables, etc., and photographs should be numbered consecutively in Arabic numerals. A short title should be provided at the bottom of each page. Photographs must be of good quality. Original charts, tables, etc., will be required for printing.
3. Foot notes or End notes may be used. But it is advisable to use parenthetical documentation as recommended by Science Citation Index (SCI) for Research papers. Notes should be worked into the text if they help clarity. References or works cited should be given at the end of the text and consolidated into a final alphabetized section.
4. All articles are, as a rule, referred to experts for peer review in the subjects concerned. Those recommended by the referees alone will be published in the Journal after appropriate editing.
5. A declaration stating that the article has not been submitted elsewhere should accompany the manuscript.
6. Submission of an article does not guarantee publication.

"ANTIBACTERIAL ACTIVITY OF MARINE MICROALGAE FROM ENAYAM COAST, WEST COAST OF INDIA"

M.Anulgan Sheril Franko*, A. Paniadima.**

Abstract

Eleven species of diatoms collected from Enayam, West Coast of India, were cultured in the laboratory under controlled conditions by using six different culture media. The Walne's and F/2 media was found to be more suitable for all the diatom species cultured. The optimum temperature for microalgal growth was found to be at 20°C. The salinity range of 25 – 28 ppt was most suitable for the algal growth. The relationship between pH and the growth of diatom were also studied. The diatoms showed the peak growth at 7.2 pH. Different solvent fractions of the diatom extracts were used to study their antibacterial activity against thirteen pathogenic bacteria. Of the six diatoms studied, Thallassiothrix frauenfeldii *showed highest activity against almost all the tested bacteria. The diethyl ether extracts were more active against most of the pathogens. The diatoms are potentially good source of new antibacterial agents.*

Introduction

The ocean is a rich source of biologically active natural products of diverse structural types (Jackson *et al* 2009). All phytoplankton are suspected to be producing toxic substances. (Guillard, 1995). Many of the potent toxins like aplysiatoxin, saxitoxin, brevitoxin etc. are produced by microalgae. The diatoms constitute a major part of the phytoplankton population and are seen to show biological activity (Pieme, *et al.* 2008). Their abundance and productivity in the sea are strongly driven by the seasonal oscillation of their physical and chemical environment. Being highly sensitive organisms, their mass production is attempted only under restricted to laboratory conditions. Over the past decade, blooms of the domoic acid producing diatom *Pseudonitzschia* have been responsible for numerous deaths of marine mammals and birds in Monteray Bay, California. Hence the study was carried out to experiment culture of marine micro algae as a rich source of biologically active substances.

* *Department of Zoology, St. Jude's College, Thoothoor PO. Kanyakumari Dist.*

** *PG & Research Department of Zoology, Alagappa Govt Arts College, Karaikudi.*

Materials And Methods

Microalgal samples were collected from Enayam of Arabian sea, southwest coast of India by towing phytoplankton net by a mechanized boat. The sample was carried to the laboratory within two hours in an insulated container with ice cubes to avoid thermal and light shock and filtered through 330 mm bolting silk to remove zooplankton. Required species of diatoms in adequate numbers were isolated by using a sharp Pasteur isolation pipette under microscope.They were repeatedly washed in sterilized water to reduce bacterial population and then cultured in the laboratory.

Diatom species were selected , identified and purified. The growth performance in the following culture media was made as per the procedure given by Guillard, (1995) and Gopinathan (1995).

1. F/2 medium
2. Walne's medium
3. Mixed culture medium
4. Schreiber's medium
5. Miquel's medium and
6. TMRL medium.

Serial dilution technique was employed to obtain pure culture of diatoms. This procedure was repeatedly followed at the end of each growth phase until a pure culture was obtained. Stock of algal species were maintained in one liter culture flasks containing 750 ml of medium under the following conditions. Light intensity, 3000 lux, provided from overhead cool white fluorescent tubes, lighting cycle, 14 hours light followed by; 10 hours darkness, temperature, 28±1 ^{o}C and salinity 29 ppt. Sub cultures were raised regularly at an interval of 4 to 7 days.

In order to find out the optimum pH at which the diatom production is highest, the diatoms were subjected to the following conditions. Walne's medium of different pH ranges were prepared to study the relation between the pH and diatom growth. In all the experiment, the inoculum was kept constant (10^4 cells L^{-1}).

Four sets of culture systems in duplicate were subjected to light and dark period of constant intensity. The experimental set ups were subjected to 6/18 hour, 12/12 hour, 18/6 hour and 24/0 hour different light and dark period respectively while keeping all other parameters constant to study the relation between the light and multiplication of microalgae (Guillard, 1995). The light intensity was

kept constant (» 5.0 $wm^{-2} s^{-1}$). The light intensity was standardized using LI-COR quantum or radiometer or photometer model LI-189, England. In order to reduce the bacterial population ampicillin was introduced in the culture system (Guillard, 1995).

The cultures were also experimentally grown in different temperatures ranging from 16°C to 36°C at a constant interval of 4°C in a specially designed growth chamber to study the optimum temperature at which the diatoms grow at its highest. Walne's medium of different range of salinity was prepared from 20 to 34 ppt by adding distilled water to decrease salinity with a range difference of 2 ppt. After the incubation period the cells were counted by using haemocytometer and their cell density was expressed as number of cells per liter.

Antibacterial Activity

Extraction of Bioactive substances from Diatoms

Non-axenic unialgae were mass cultured in the above mentioned six media in the laboratory and filtered at the early stationary growth phase (Viso *et al*., 1987). The harvested algal cells were washed with tap water, air dried and then homogenized to fine powder and was stored in airtight bottles for further analysis. Aqueous and solvent extraction was carried out based on the procedure given by Nair *et al*. (2004). The solvents like diethyl ether, methanol, acetone and chloroform. were used for the extraction of bioactive compounds from the diatoms. The collected fractions of the four solvents were tested for their antibacterial activity against the eleven pathogenic bacteria. Disc diffusion method was followed to study the antibacterial activity (Salie *et al*. 1996). Sterile filter paper discs, 5 mm in diameter, were impregnated with 0.05 ml of the extract and dried at room temperature. The prepared discs were stored in a refrigerator over calcium chloride (Manivasagam *et al*. 1991) until they were used. Filter paper treated with the solvents like diethyl ether, methanol, acetone and chloroform were used and tetracycline drug was served as standard.

Result

Eleven species of diatoms were cultured successfully in the laboratory under controlled conditions. They are *Biddulphia mobilensis, Chaetoceros lorenzianus, Climacosphenia moniligera, Coscinodiscus excentricus, Fragilaria oceanica, Leptocylindrus danicus, Navicula longa, Nitzschia sigma, Pleurosigma angulatum, Skeletonema costatum* and *Thallassiothrix frauenfeldii.* The results showed that the algae grown in Walne's medium (683 to 5628 x 10^3) and F/2 medium (598 to 4638 x 10^3) grew better than those were cultured in other media. The lowest algal growth (2 to 314.6 x 10^3) was recorded in the SC medium (Fig. 1).

The highest growth of algae was noted when they were kept between 20°C (614 to 4716 x 10^3 cells) to 24°C (602 to 5328 x 10^3 cells). Temperature above 32°C, did not show any growth. At 28°C, the growth was found to be reduced approximately 50% when compared to growth at 20°C. At 36°C, all the diatoms died (Fig. 2).

The algae attained the highest growth at 24/0 hour light and dark in an average of two days. It took four days at 18/6 hour light and dark; seven days at 12/12 hour light and dark and eighteen days at 6/18 hour light and dark. The stock cultures were maintained at 20°C under 6/18 hour light and dark which was found viable for 20 – 26 days (Fig. 3 to 6).

The marine species of diatoms grew well at ≈ 28 to 32 ppt salinity. The growth was found to decrease at a salinity below 28 ppt and above 32 ppt. No growth was recorded above 34 ppt and below 20 ppt (Fig. 7 and 8).

The diatoms showed their peak growth at pH 7.2. *P. angulatum* and *C. moniligera* amounted to 16.45 x 10^6 cells/litre and 16.94 x 10^6 cells/litre respectively. But at 8.2 pH, they produced 3.14 x 10^5 and 4.82 x 10^5 cells per litre respectively after a growth period of 96 hour (Fig 9).

Antibacterial Activity

Six species of diatoms were screened against thirteen pathogenic bacterial strains. Among them, two were gram positive and the rest were gram negative. Among the two gram positive bacteria, *Bascillus subtilis* (BS) and *Staphylococcus aureus* (SA), the latter was comparatively more susceptible (Table 1). Of the gram negative bacteriae *Salmonella paratyphi-b* (SP), *S. typhi* (ST) and *Pseudomonas aeroginosa* (PA) were least resistant strains. *Enterobacter aerogenes* (EA), *Acinitobactor calcoaceticus* (AC), *and Shiegella sp.* (SS) were highly resistant strains and the resistance increased from *Escherischia coli* (EC), *Vibrio cholerae* (VC), *Vibrio parahaemolyticus* (VP), *Klebsiella pneumoniae* (KP) and *Proteus mirabilis* (PM).

Of the six diatoms studied, *Thallassiothrix frauenfeldii* showed highest activity against almost all the bacteria tested followed by *Chaetoceros lorenzianus, Pleurosigma angulatum, Nitzschia sigma, Leptocylindrus danicus and Biddulphia mobilensis*. The tested species were fractionated with organic solvents like Diethyl ether, Acetone, Chloroform and Methanol and the different fractions were tested independently against the bacterial strains (Table 1), (Fig.10).

Of all the four solvents tested, the highest activity was shown by the diethyl ether fraction; moderate activity was shown by the acetone and chloroform fractions, while methanol fraction produced only a trace or negligible zone of inhibition against the tested microbes. Aqueous fractions (control) never showed any response to the tested pathogens (Fig.10).

Table 1:

Antibacterial Action Of Different Solvent Fractions Of Six Diatom Sp.
The Values Given Are Zone Of Inhibition In Mm

Algae	Solvent	Gram +ve		Gram –ve										
		BS	SA	AC	EA	EC	KP	PM	PA	SP	ST	SS	VC	VP
Biddulphia	Dieth .E	8	8	-	-	6	4	2	8	9	9	-	6	4
mobilensis	Act	6	7	-	-	5	2	Tr	7	9	8	-	3	1
	Chl	6	6	-	-	2	-	-	7	7	7	-	3	-
	Met.	3	2	-	-	-	-	-	-	Tr	-	-	2	-
Chaetoceros	Dieth .E	10	10	Tr	Tr	9	3	2	7	9	6	Tr	9	6
lorenzianus	Act	8	6	Tr	-	4	Tr	-	7	8	4	Tr	4	2
	Chl	8	5	-	-	4	-	-	4	Tr	4	-	4	2
	Met.	4	-	-	-	-	-	-	-	-	-	-	-	1
Leptocylindrus	Dieth .E	4	5	-	-	4	2	Tr	3	6	4	-	4	5
danicus	Act	3	4	-	-	3	2	Tr	1	5	4	-	2	2
	Chl	4	4	-	-	3	Tr	-	1	5	3	-	2	1
	Met.	2	2	-	-	-	-	-	-	Tr	3	-	-	-
Nitzschia	Dieth .E	6	11	Tr	1	8	2	1	13	8	6	1	2	4
sigma	Act	3	7	-	Tr	6	Tr	Tr	9	6	4	1	1	2
	Chl	2	7	-	Tr	6	-	-	7	6	3	Tr	-	-
	Met.	2	-	-	-	Tr	-	-	2	1	-	-	-	-
Pleurosigma	Dieth .E	8	9	-	-	7	3	2	8	9	8	-	6	4
angulatum	Act	6	6	-	-	6	2	Tr	8	7	7	-	2	Tr
	Chl	5	4	-	-	6	Tr	Tr	6	7	7	-	-	-
	Met.	-	4	-	-	-	-	-	2	-	5	-	-	-
Thallassiothrix	Dieth .E	8	11	2	2	12	3	4	7	5	9	Tr	7	5
frauenfeldii	Act	6	6	Tr	1	7	-	4	6	4	7	Tr	4	2
	Chl	4	2	-	-	7	-	1	2	1	5	-	4	-
	Met.	-	2	-	-	-	-	-	-	-	-	-	-	-

Dieth.E : Diethyl ether Act: Acetone Chl : Chloroform Met.: Methanol

Tr : Trace = < 1 mm

Controls were not mentioned in the table since they showed no measurable activity.

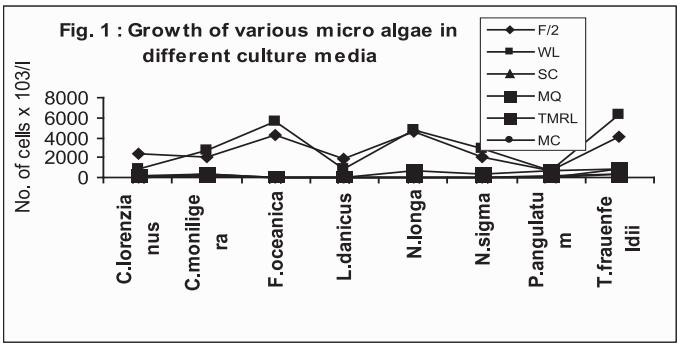
Fig. 1 : Growth of various micro algae in different culture media
F/2
WL
SC
MQ
TMRL
MC
No. of cells x 103/l
8000
6000
4000
2000
0
C.lorenzianus
C.monilifera
F.oceanica
L.danicus
N.longa
N.sigma
P.angulatum
T.frauenfeldii

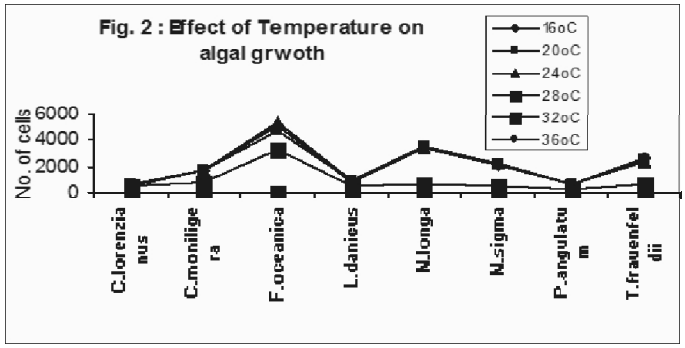
Fig. 2 : Effect of Temperature on algal grwoth
16oC
20oC
24oC
28oC
32oC
36oC
No. of cells
6000
4000
2000
0
C.lorenzianus
C.monilifera
F.oceanica
L.danicus
N.longa
N.sigma
P.angulatum
T.frauenfeldii

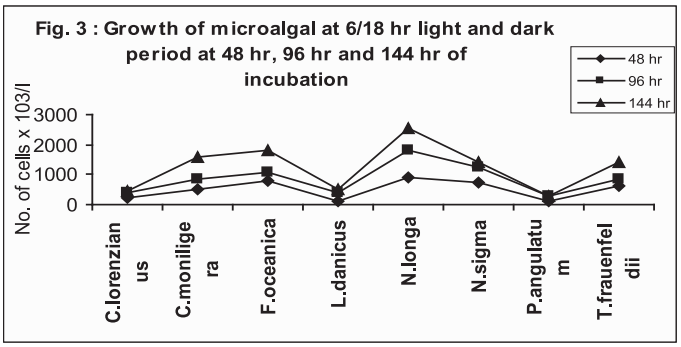
Fig. 3 : Growth of microalgal at 6/18 hr light and dark period at 48 hr, 96 hr and 144 hr of incubation
48 hr
96 hr
144 hr
No. of cells x 103/l
3000
2000
1000
0
C.lorenzianus
C.monilifera
F.oceanica
L.danicus
N.longa
N.sigma
P.angulatum
T.frauenfeldii

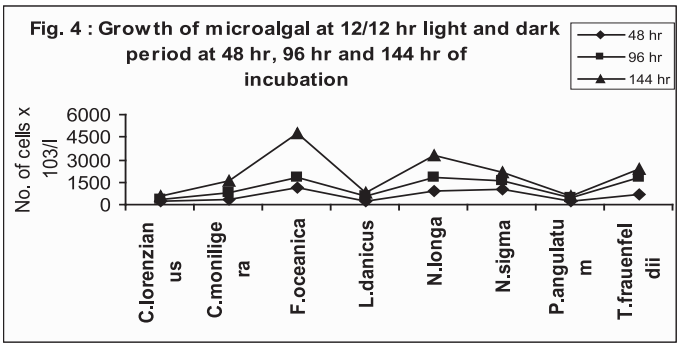
Fig. 4 : Growth of microalgal at 12/12 hr light and dark period at 48 hr, 96 hr and 144 hr of incubation
48 hr
96 hr
144 hr
No. of cells x 103/l
6000
4500
3000
1500
0
C.lorenzianus
C.monilifera
F.oceanica
L.danicus
N.longa
N.sigma
P.angulatum
T.frauenfeldii

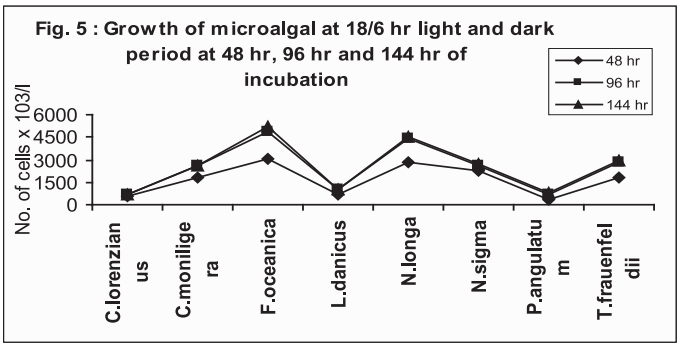
Fig. 5 : Growth of microalgal at 18/6 hr light and dark period at 48 hr, 96 hr and 144 hr of incubation
48 hr
96 hr
144 hr
No. of cells x 103/l
6000
4500
3000
1500
0
C.lorenzianus
C.monilifera
F.oceanica
L.danicus
N.longa
N.sigma
P.angulatum
T.frauenfeldii

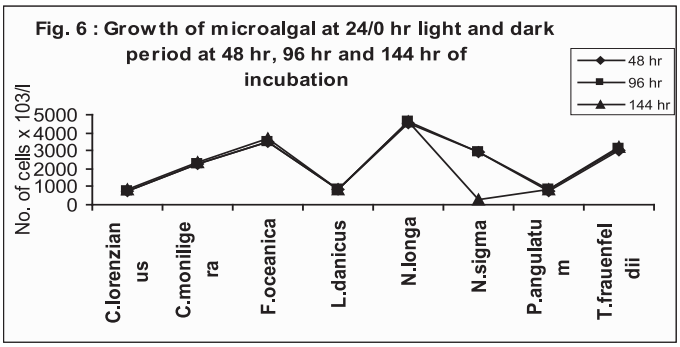
Fig. 6 : Growth of microalgal at 24/0 hr light and dark period at 48 hr, 96 hr and 144 hr of incubation
48 hr
96 hr
144 hr
No. of cells x 103/l
5000
4000
3000
2000
1000
0
C.lorenzianus
C.monilifera
F.oceanica
L.danicus
N.longa
N.sigma
P.angulatum
T.frauenfeldii

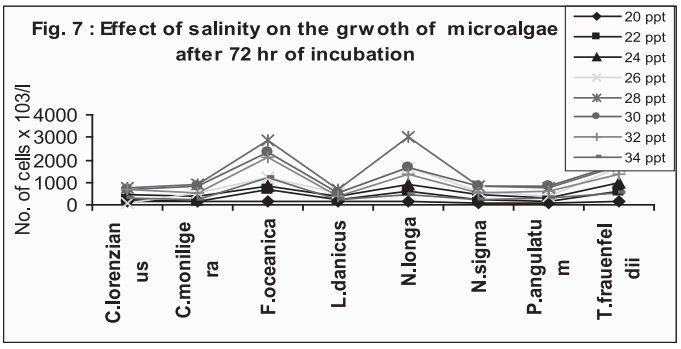
Fig. 7 : Effect of salinity on the grwoth of microalgae after 72 hr of incubation
20 ppt
22 ppt
24 ppt
26 ppt
28 ppt
30 ppt
32 ppt
34 ppt
No. of cells x 103/l
4000
3000
2000
1000
0
C.lorenzianus
C.monilifera
F.oceanica
L.danicus
N.longa
N.sigma
P.angulatum
T.frauenfeldii

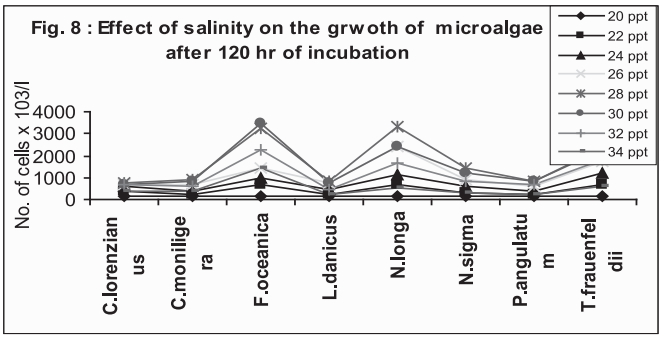
Fig. 8 : Effect of salinity on the grwoth of microalgae after 120 hr of incubation
20 ppt
22 ppt
24 ppt
26 ppt
28 ppt
30 ppt
32 ppt
34 ppt
No. of cells x 103/l
4000
3000
2000
1000
0
C.lorenzianus
C.monilifera
F.oceanica
L.danicus
N.longa
N.sigma
P.angulatum
T.frauenfeldii

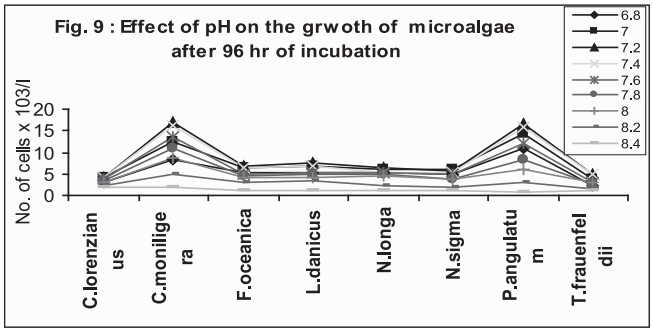
Fig. 9 : Effect of pH on the grwoth of microalgae after 96 hr of incubation
6.8
7
7.2
7.4
7.6
7.8
8
8.2
8.4
No. of cells x 103/l
20
15
10
5
0
C.lorenzianus
C.monilifera
F.oceanica
L.danicus
N.longa
N.sigma
P.angulatum
T.frauenfeldii

Discussion

Six different culture media were used in the laboratories for microalgal culture around the world. In the present investigation, (Walne's medium and F/2 medium were found very suitable to grow all the eleven species of diatoms, which were found to be abundant in the near shore of Kerala and Madras Coasts. The size of the diatoms were found to be diminishing when they were frequently transferred to fresh culture media while maintaining the culture in the laboratory (Guillard1995). At one stage, they stopped multiplication.

Temperature is one of the major factors which control the growth of microalgae in culture media (Gopinathan, 1995). Illumination is another factor controlling the growth of microalgae (Guillard 1995).From the result of the present investigation, it was understood that under optimal conditions, the duration of light is inversely proportional to the time taken for attaining the peak growth (Fig.3 to 6).

It was found that there was definitely a major effect of salinity over the growth and multiplication of diatoms. The optimum range was found to be 28 to 32 ppt and it varies from species to species (Fig.7 and 8). pH also has a control over the diatom growth was negatively affected (Guillard1995). At pH 8.2 , highest bacterial population was noticed (Fig.9).

Ampicillin 0.4 mg l^{-1} was added to check the bacterial population. The diatom collected from antibiotics added culture media was not used for the bioactivity studies, since it was assumed that the impact of antibiotics may influence the bioactivity. Diethylether extracts showed highest activity against most of the tested pathogenic bacteria. Acetone and chloroform extracts showed only moderate activity while methanol fraction showed negligible activity and the aqueous fraction never showed any activity (Table 1). The diethyl ether extract of *Thallassiothrix frauenfeldii* showed maximum activity against all the tested bacterial strains. It was followed by *Nitzschia sigma* and *Chaetoceros lorenzianus*. The maximum activity was noticed on the same extract of *Leptocylindrus danicus*. Generally *Actinobactor calcoaceticus, Enterobacter aerogenes, Shiegella sp.and Proteus mirabilis* were resistant against most of the extracts of diatoms tested. The diethylether is very effective in extracting the antibacterial substances from the microalgae. It is because diethylether has a low density, low viscosity, high evaporating capacity and low boiling point when compared to the remaining solvents as reported by Kannapiran and Nithyanandan (2002).

Antibiotics produced by microorganisms inhibit the growth or activity of other micro organisms. Most of the infectious diseases can be brought under control with natural or synthetic drug products. Many marine algal species were found to have growth inhibiting effect on bacteria, fungi, virus etc. (Rao, 1998).

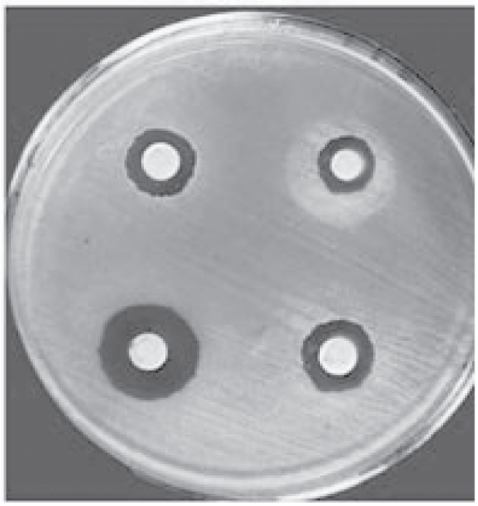

Nitzschia sigma

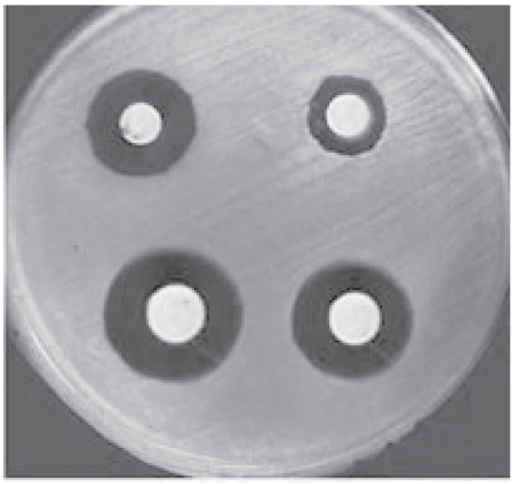

Pleurosigma angulatum

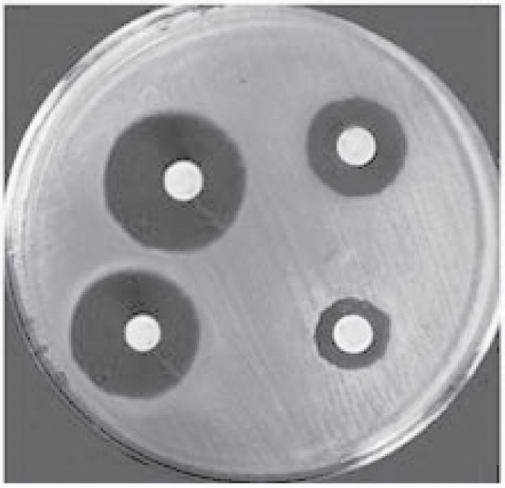

Chaetoceros lorenzianus

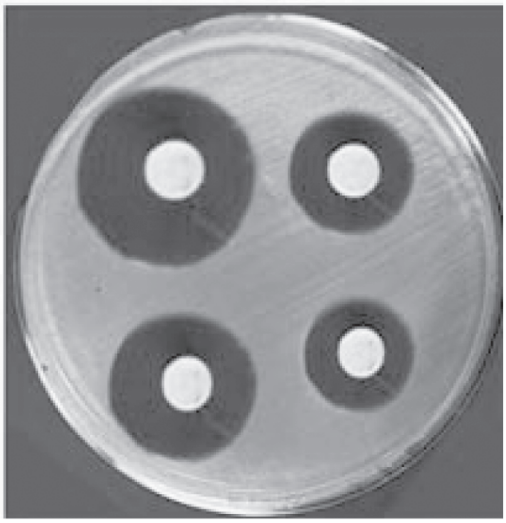

Thallossiothrix frauenfeldii

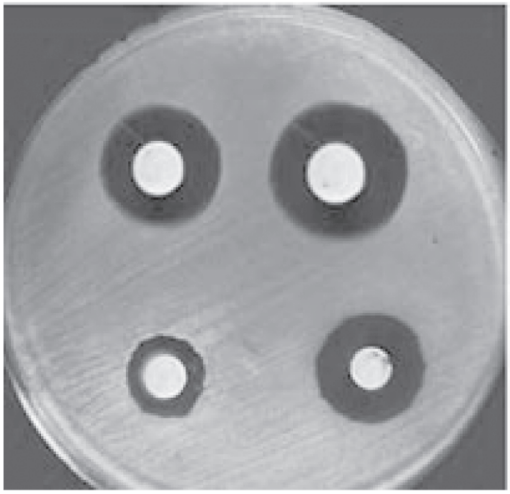

Leptocylindrus danicus

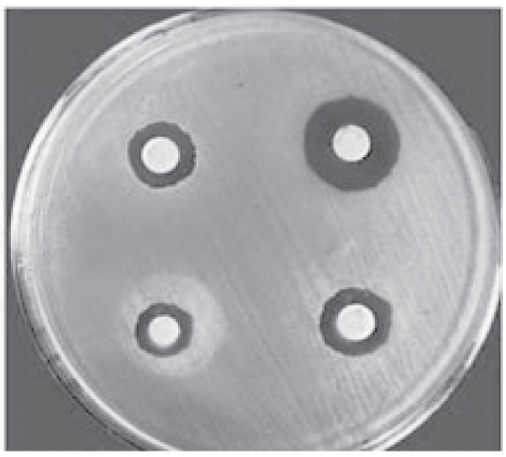

Biddulphia mobilensis

Fig.10 Bio-activity by Diethyl Ether Fraction

Certain marine microalgae have long been investigated extensively to isolate life saving drugs or biologically active substances from all over the world. .(Rao, 1998). Antimicrobial substances derived from marine planktonic algae, consists of diverse groups of chemical compounds.These include bromophenols, tarpenes, methyolated fatty acids , neuro toxins, goniodomin, saxitoxin, brevitoxin, Belta-diketone , acrylic acid , lipoprotein, poly saccharides etc.(Pesando,1990).

The marine planktonic algae would become a source of new drugs of potential commercial value. The knowledge of the presence of antibacterial activity in natural seawater may be one of the reasons of man to turn back towards the sea for potential drugs as reported by Pesando, (1990) and Paniadima (2007).

The results indicate that marine microalgae are potentially good source for new antibacterial agents and that organic solvent extraction of algal biomass appears to the most effective means of isolation of compounds as reported by Pesando (1990). The information obtained in this study could be used for isolating bioactive compounds. These compounds should further be identified & tested *invivo* for toxicity and other physiological responses. These compounds could be synthesized or isolated from the algae itself. Antifertility studies and other behavioural studies should be conducted before coming to a conclusion to use these products as drugs for diseases

References

1. Gopinathan, C.P., (1995). Microalgal culture – part I. Live Feed hand book on aquatic organism, MPEDA pp.14-17.
2. Guillard, R.R.L., (1995). Culture methods : In Manual on harmful marine micro algae (Ed. G.M.Hallegraff, D.M. Anderson, A.D.Cambella) I.O.C. Manuals and Guides No.33, p.45-62.
3. JacksonC., Agboke A and V.Nwoke, (2009). *In vitro* evaluation of microbial activity of combinations of nystatin and *Euphorbia hirta* leaf extract against *Candida albicans* by the checkerboard method. Journal of Medicinal Plants Research.4.(4), 1228-1230.
4. Kannapiran, E. and M. Nithyanandan, (2002). Antibacterial activity of different fractions of extracts from Palk Bay seaweeds. Seaweed Res. Utiln. 24(1): 177 – 181.
5. Manivasagam, S., A. Selvaraj, A. Purushothaman and A.Subramanian, (1991). Light induced antibacterial activity of diatom, *Pleurosigma elongatum*. Eds. Thompson, M.F., R.Sarojini; R.Nagathushnam. In Bioactive compounds from marine organisms with emphasis on the Indian Ocean – An Indo. US Symposium. Oxford & IBH Publ. Co. Pvt. Ltd., New Delhi, pp. 263 – 266.
6. Nair R, T. Kalariya and S. Chanda, (2004). Antibacterial activity of some selected Indian medicinal flora. Turk J Biol 29: 41-47.
7. Padmini Sreenivasa Rao , (1998). Biological investigation of Indian Phaeophyceae XVII. Seasonal variation of antimicrobial activity of total Sterols obtained from frozen samples of *Sargassum johnstonii* Setchell

et Gardener. Seaweed Res.Utiln.,20 (1&2):91-95

8. Paniadima., (2007). Studies on the structure and dynamics of Plankton Community of Enayam Coast, West Coast of India, Ph.D. Thesis, Alagappa University, pp. 116-137.
9. Pesando, D., (1990). Antibacterial and antifungal activities of Marine Algae, Ed. 1. Akatsugo. In introduction to Applied Phycology. SPB Academic Publ. Br, the Hague, the Netherlands. 3 – 26.
10. Pieme C A., Dzoyem J P., Kechia F A., Ethoa F X and V.Penlap , (2008). *In vitro* antimicrobial activity of extracts from some Cameroonian medicinal plants.Journal of Biological sciences 8(5) 902-907.
11. Salie, F., P.F.K. Eagles and H.M.J. Leng, (1996). Preliminary antimicrobial screening of four South African Asteraceae species. J Ethanopharmacol 52: 27-33.
12. Viso, A.C., D. Pesando and C. Bay, (1987). Antibacterial and antifungal properties of some marine diatoms in culture. Bot. Mar. 30: 41 – 45.

COMPUTING MEDIAN WITH DATA DEPTH IN MULTIVARIATE DATA

Muthukrishnan.R* and **Poonkuzhali.G****

Abstract

Depth is an integer assigned to be a candidate fit for relative to a data set. A data depth can be used to measure the depth or outlyingness of a given multivariate sample with respect to its underlying distribution. This leads to outside-inward/centre-outward ordering of the sample points. Many graphical and quantitative methods are well-established for analysing the measures such as location, scale and shape, as well as comparing inference methods based on data depth. The notion of depth, first proposed by Tukey[16], is a multivariate median which is the deepest point in a given data cloud. Donoho and Gasko[2] applied hyperplanes approach to determine depth using smallest portion of data that are separated by a hyperplane. Since then, many depths procedures have been established and rich statistical methodology has been developed. During the last decade the notion of depth received more attention from the research community due to availability of high speed personal computers. The selection of depth statistic in applications is the question of computability and robustness. The computational aspect of depth in higher dimensions is still a challenging task for the researchers. This paper explores the various depth procedures. Also, the performance of these procedures has been studied by computing median/centre under real and simulating environment with the help of R package.

Keywords

Depth – Real data – Simulation Study – R package.

1. Introduction

Data depth is an important concept of multivariate data analysis. Depth based methodology in both univariate and multivariate cases may be based on idea of ranks. In univariate case linear ranking is used, that is smallest to largest while in multivariate case centre-outward ordering. This

**Assistant Professor, Department of Statistics, Bharathiar University, Coimbatore-641046. E-mail: muthukrishnan1970@gmail.com*

*** Research Scholar, Department of Statistics, Bharathiar University, Coimbatore-641046. E-mail: poostat18@gmail.com*

ordering provides an understanding of a related notion of centre and the points near the centre should have higher depth. The usual order statistics is different from the depth order statistics. In usual order statistics the data are ordered from the smallest sample point to the largest, while in depth order statistics it starts from the middle sample point and move outwards in all directions.

Using different notions of data depth, one can compute depth values for all sample points in the data cloud. The data point with the highest depth is called the deepest or central point or simply centre. The data point with lowest depth value is called the most outlying point. If more than one sample point is present with highest depth, the average of them is considered as the deepest point. The depth should assume higher values when the given point is near the centre of the distribution and should tend to zero as the points move away from the centre.

Based on this ordering of depth one can compute descriptive statistical measures such as multivariate location, scale, skewness and kurtosis**.** The depth related graphical displays such as Contour plot, Bag plot, Sunburst plot, Perspective plot, DD plot, Blotched bag plots can be used for analyzing the distributional characteristics of the multivariate data cloud.

Tukey[16] proposed halfspace depth and recommended its role in multivariate analogues of univariate rank. Based on halfspace depth, Donoho and Gasko[2] described multivariate location estimators. Yeh and Singh[18] proposed method for constructing confidence regions. A depth based rank sum statistic for multivariate data was initiated by Liu and Singh[5]. Rousseeuw et al.[12] and Liu et al.[3] formulated depth related graphical displays for data analysis. Rousseeuw and Hubert[11] initiated a notion of depth in the regression context. It provides the rank of any plane, rather than ranks of observations. More details about the depth function and its properties are given in Zuo and Serfling[21] and monography by Mosler[8]. A class of projection based depth functions were introduced by Zuo[22]. Comprehensive reviews on data depth are given in Serfling[14], Liu et al.[6], Cascos [1] and Mosler [9] described both theoretical as well as applied work.

In section 2, various existing notions of data depth are defined and the desirable properties of statistical depth function are also listed. The performance of the various depth procedures have been carried out by computing median and the corresponding depth value on real and simulation and data thus the obtained results are summarized in section 3. The section 4 discusses the conclusions of the study.

2. Materials and Methods

Many procedures have been established to find location measure by computing its depth value in the data cloud. The general notion of various data depth and the properties are summarised in this section.

2.1 The various notions of Data depth

A depth procedure induces a family of central regions. There are various procedures to find depth value for each given point in the data cloud. The celebrated depth procedures are based on conventional mean vector and dispersion matrix, projection based, and also, median and median absolute deviation. This section provides an overview of the various depth procedures which are used to find the deepest point in a data cloud.

The Mahalanobis depth (Mahalanobis[7]). This depth studies the elliptical structure of a multivariate distribution. Let $X = X_1, X_2, ..., X_p$ be a p dimensional multivariate data cloud X in R^p and let $d(\mathrm{x}, \mu_F)$ be the Mahalanobis distance between the arbitrary point $\mathrm{x} \in R^p$ and μ, the mean vector of data cloud.

$$d(\mathrm{x}, \mu) = (\mathrm{x} - \mu)' \Sigma^{-1} (\mathrm{x} - \mu)$$

where μ and Σ are the mean vector and dispersion matrix of data cloud in R^p respectively. The Mahalanobis depth at arbitrary point x is defined as

$$M_n D(\mathrm{x}, X) = [1 + d(\mathrm{x}, \mu)]^{-1}$$

and its sample version is obtained by replacing μ and Σ with their sample estimates $\bar{X}$ (sample mean) and s (sample dispersion matrix).

The Halfspace depth (Tukey[16]). It reflects a generalization of the notion of ranks to multivariate data. For univariate case**,** given some number x, all values less than or equal to x is a closed halfspace, and all points less than x is an open halfspace. Similarly, all points greater than or equal to x form a closed halfspace and all points greater than x is an open halfspace**.** In multivariate case, for general p-variate, consider any point x (a column vector) having length p, let н be any closed halfspace containing the point x, and let p(н) be the probability be associated with н. That is, p(н) is the probability that an observation occurs in the halfspace н. Then, the halfspace depth of the point x is the smallest value of p(н) among all halfspaces н containing x. Tukey's halfspace depth is

$$HD = \inf_{\mathrm{H}} [p(H) : H \ is \ a \ closedhalf \ space \ containing \ \mathrm{x}]$$

For p>1, halfspace depth can be defined instead as the least depth of any one-dimensional projection of the data (Donoho and Gasko [2]).The procedure for computing Halfspace depth is elaborately given in Wilcox[20] (pg. 218-221).

The Oja depth (Oja[10]). It is based on average volumes of simplices not based on distances. Let x is any arbitrary point in the data cloud X, ch is the convex hull, V_d is the d-dimensional volume, Σ the covariance matrix, then Oja depth is defined as

$$OD(\mathrm{x}, X) = \left(1 + \frac{E(V_d(ch\{Z, X_1, X_2, ..., X_d\}))}{\sqrt{\det \Sigma}}\right)^{-1}$$

The Simplicial depth (Liu[4]). This depth emerges naturally out of a fundamental concept underlying affine geometry, namely that of a simplex, and it satisfies the requirements on would expect from a notion of data depth. The simplicial depth of an arbitrary point x in data cloud X is defined as

$$SD(\mathrm{x}, X) = P\left(\mathrm{x} \in S\left[\mathrm{x}_1,...,\mathrm{x}_{p+1}\right]\right)$$

where x is a random sample from X and $S[x_1,...,x_{p+1}]$ denotes the p-dimensional simplex with vertices $x_1,...,x_{p+1}$ that is the set of all points in the data cloud.

The Projection depth (Zuo and Serfling[21]). Its induced estimators are very favourable because they can enjoy very high breakdown point robustness without having to pay the price of low efficiency meanwhile providing a promising centre-outward ordering of multidimensional data. The computation of projection depth seems intractable since it involves supremum over infinitely many direction vectors. Let u be any p-dimension vector having unit norm. x is an any arbitrary point in the data cloud X , Med denotes the Median of data cloud X, MAD denotes the Median Absolute Deviation. Then projection depth is defined as

$$PD(\mathrm{x}, X) = \left[1 + \sup_{\|u\|=1} \frac{\left|u'\mathrm{x} - Med(\mathrm{x}, \mathrm{X})\right|}{MAD(\mathrm{x}, \mathrm{X})}\right]^{-1}$$

The L^p depth. (Zuo and Serfling[21]). This depth can be measured by a distance from a properly chosen center of the data cloud. Different distances (norms) relative to the underlying data cloud were treated with equal importance that is equally weighted. It is defined as

$$L^p D(\mathrm{x}, \mathrm{X}) = \left(1 + E\left\|\mathrm{x} - \mathrm{X}\right\|_p\right)^{-1}$$

For p=2, $\widetilde{L}^2 D(\mathrm{x}, \mathrm{X}) = \left(1 + E\left[\left\|\mathrm{x} - \mathrm{X}\right\|_{\Sigma^{-1}}\right]\right)^{-1}$

where Σ is the covariance matrix of X.

L_1-median/Euclidean median (Weiszfeld[19]). This procedure is a robust estimator of multivariate location with good statistical properties. It is also called geometric median. Let $X_1, X_2,..., X_p$ be a P dimensional multivariate data cloud in R^p then L_1 median of the set of points $X_1, X_2,..., X_p$ to any point $\overline{\mu} \in R^p$ which minimizes

$$\arg\min_{\mu} \sum_{i=1}^{n} \left\|X_i - \mu\right\|$$

where $\left\|X_i - \mu\right\|$, the Euclidean distance between X_i and μ in R^p. In words, the L_1 median is the point for which the sum of the Euclidean distances to given data points is minimal.

2.2 Desirable Properties

The various desirable properties of depth procedure have been consolidated by Zuo and Serfling[21] and are briefly furnished below.

(i). Affine invariant: The depth of a point $x \in R^p$ should not depend on the fundamental coordinate system or in particular on the scales of the fundamental measurements. In notation,

$D(Ax+b) = depth(x;X)$ for every b and every non singular linear transformation A

(ii). Maximality at centre: For a distribution having a uniquely distinct centre, the depth function should attain maximum value at this centre.

$D(\vartheta, X) = \sup_{x \in R^d} D(x;X)$ having centre ϑ

(iii). Monotonicity relative to deepest point: As a point $x \in R^p$ moves away from the deepest point along any fixed line through the centre, the depth at x should decrease monotonically. For any X having deepest point, $D(x;X) \le D(\vartheta + \alpha(x-\vartheta) : X)$ holds for $\alpha \in [0,1]$

(iv). Vanishing at infinity: The depth of a point x should move towards zero as $\|x\|$ approaches to infinity.

$D(x:X) \to 0$ as $\|x\| \to \infty$

The established depth procedures, specifically Oja, Halfspace and Projection based procedures follows the properties such as affine invariant, maximality at centre, monotonicity relative to the deepest point and vanishing at infinity. Simplicial depth satisfied the properties like affine invariant and vanishing at infinity. Also it satisfied the properties maximality at centre and monotonicity relative to the deepest point in continuous distribution but not necessarily discrete symmetric distribution. $\mathbf{L^p}$ depth satisfied the properties maximality at centre, monotonicity relative to the deepest point, vanishing at infinity and it satisfied affine invariant under the conditions of rotational and rigid body transformations. Mahalanobis depth satisfied all the four properties but median generated by the Mahalanobis depth depends critically on the choice of location covariance measures.

3. Result and Discussion

This section presents the comparison of various notions of depth by computing median and its depth value along with classical and Euclidean median. The experiments were carried out under real and simulating environment with the help of packages in R.

3.1 Real data

The efficiency of the various notions of depth is executed in a real data set. The famous starsCYG data set was considered. The data set contains 47 observations of 2 variables. The

computed median and its depth values under the various methods are displayed in the table 1. The scatter plot with located median/centre under various depth based procedures is displayed in the figure 1.

Table 1. Computed Median and its Depth value

Procedures	Median	Depth
Mahalanobis	4.38,5.02	0.94
Halfspace	4.38,4.96	0.40
Oja	4.40,5.02	0.47
Simplicial	4.45,5.22	0.31
Projection	4.38,5.02	0.65
L^p	4.38,5.02	0.41
Classical	4.42,5.10	
Euclidean	4.40,5.04	

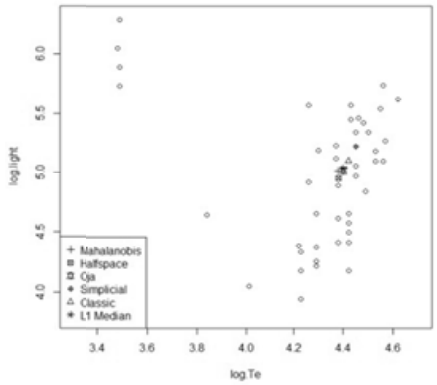

Figure1. Median with various depth procedures

The results reveals that, median induced by Oja depth represents the Euclidean median and others are also almost similar to Euclidean except simplicial depth.

3.2 Simulation

A simulation study is also performed to compare the efficiency of the various notions of depth procedures. The data points are simulated from multivariate normal distribution. The experiments were performed with the simulated bivariate data with mean vector (5, 5) and the covaraiance matrix (1,0,0,1) under the sample sizes 100, 1000, 5000 and 10000. Again the same study was conduted for the contaminated situation. The various levels of contamination such as 1%, 2%, 5%, 10% and 20% were considered. The computed median along with the depth value under various methods are displayed in the table 2.

Table.2 Computed Median and its Depth Value

Procedures	Median (n=100)					
	e=0.0	e=0.01	e=0.02	e=0.05	e=0.1	e=0.2
Mahalanobis	5.01,4.93 (.9)	5.01,4.93 (.9)	5.01,4.93 (.9)	5.54,5.37 (.9)	5.51,5.54 (.9)	6.32,6.47 (.9)
Halfspace	5.01,4.93 (.4)	5.01,4.93 (.4)	5.01,4.93 (.4)	5.01,4.93 (.4)	5.46,5.06 (.4)	5.54,5.37 (.9)
Oja	5.08,4.97 (.3)	5.08,4.98 (.3)	5.08,4.98 (.3)	5.13,4.98 (.2)	5.23,5.07 (.2)	5.49,5.33 (.2)
Simplicial	5.01,4.93 (.2)	5.01,4.93 (.2)	5.01,4.93 (.2)	5.01,4.93 (.2)	5.46,5.06 (.2)	5.54,5.37 (.2)
Projection	5.01,4.93 (.7)	5.01,4.93 (.7)	5.01,4.93 (.7)	5.01,4.93 (.7)	5.01,4.93 (.7)	5.54,5.37 (.7)
L^p	5.01,4.93 (.2)	5.01,4.93 (.2)	5.01,4.93 (.1)	5.21,5.44 (.1)	5.51,5.54 (.1)	6.32,6.47 (.0)
Classic	5.13,5.05	4.95,4.98	4.95,4.98	4.99,4.98	5.12,5.13	5.49,5.46
Euclidean	5.04,4.94	5.06,4.97	5.05,4.99	5.09,5.00	5.19,5.09	5.44,5.32

Procedures	Median (n=1000)					
	e=0.0	**e=0.01**	**e=0.02**	**e=0.05**	**e=0.1**	**e=0.2**
Mahalanobis	4.98,5.03 (.9)	5.03,5.10 (.9)	5.13,5.12 (.9)	5.31,5.30 (.9)	5.49,5.55 (.9)	6.14,6.13).9)
Halfspace	4.98,5.03 (.4)	4.98,5.03 (.4)	5.09,5.03 (.4)	5.13,5.12 (.4)	5.13,5.12 (.4)	5.37,5.37 (.4)
Oja	5.02,5.01 (.3)	5.03,5.03 (.3)	5.04,5.05 (.3)	5.08,5.09 (.2)	5.13,5.17 (.2)	5.35,5.36 (.2)
Simplicial	4.98,5.03 (.2)	4.98,5.03 (.2)	5.03,5.10 (.2)	5.03,5.10 (.2)	5.13,5.12 (.2)	5.31,5.30 (.2)
Projection	4.98,5.03 (.9)	5.09,5.03 (.9)	4.98,5.03 (.8)	5.03,5.10 (.8)	5.13,5.12 (.8)	5.37,5.37 (.8)
L^p	4.98,5.03 (.2)	5.03,5.10 (.2)	5.13,5.12 (.2)	5.31,5.30 (.1)	5.49,5.55 (.1)	6.00,6.11 (.0)
Classic	5.03,5.01	5.04,5.03	5.06,5.05	5.09,5.09	5.13,5.16	5.35,5.36
Euclidean	5.02,5.01	5.03,5.03	5.05,5.05	5.08,5.09	5.12,5.16	5.31,5.33
Procedures	Median (n=5000)					
	e=0.0	**e=0.01**	**e=0.02**	**e=0.05**	**e=0.1**	**e=0.2**
Mahalanobis	5.01,4.97 (.9)	5.07,4.99 (.9)	5.09,5.08 (.9)	5.26,5.20 (.9)	5.55,5.50 (.9)	5.96,5.92 (.9)
Halfspace	5.02,4.97 (.4)	5.02,4.97 (.4)	5.02,4.97 (.4)	5.11,5.01 (.4)	5.17,5.10 (.4)	5.33,5.26 (.4)
Oja	5.02,4.96 (.3)	5.03,4.96 (.3)	5.04,4.98 (.3)	5.09,5.02 (.2)	5.15,5.10 (.2)	5.33,5.27 (.2)
Simplicial	5.61,3.98 (.1)	4.02,4.32 (.1)	5.28,3.82 (.1)	4.60,3.89 (.1)	4.45,6.15 (.1)	4.67,3.98 (.1)
Projection	5.02,4.97 (.9)	5.02,4.97 (.9)	5.02,4.97 (.9)	5.11,5.01 (.9)	5.17,5.10 (.8)	5.33,5.29 (.8)
L^p	5.01,4.97 (.2)	5.07,4.99 (.2)	5.09,5.08 (.2)	5.26,5.20 (.1)	5.52,5.43 (.1)	5.99,5.99 (.0)
Classic	5.02, 4.97	5.03,4.97	5.05,4.99	5.09,5.03	5.17,5.13	5.33,5.28
Euclidean	5.02,4.96	5.03,4.96	5.04,4.98	5.09,5.02	5.14,5.10	5.29,5.24
Procedures	Median (n=10000)					
	e=0.0	**e=0.01**	**e=0.02**	**e=0.05**	**e=0.1**	**e=0.2**
Mahalanobis	5.00,5.01 (.9)	5.08,5.06 (.9)	5.08,5.09 (.9)	5.25,5.24 (.9)	5.48,5.48 (.9)	6.00,5.99 (.9)
Halfspace	5.00,5.01 (.4)	5.00,5.01 (.4)	5.02,5.05 (.4)	5.08,5.06 (.4)	5.14,5.16 (.4)	5.36,5.38 (.4)
Oja	5.00,5.01 (.3)	5.01,5.02 (.3)	5.02,5.03 (.3)	5.06,5.07 (.2)	5.13,5.15 (.2)	5.33,5.34 (.2)
Simplicial	5.35,4.59 (.0)	3.49,6.25 (.0)	4.31,4.68 (.0)	5.10,5.66 (.0)	6.26,5.23 (.0)	3.32,4.28 (.0)
Projection	5.00,5.01 (.9)	5.00,5.01 (.9)	5.02,5.05 (.1)	5.08,5.09 (.9)	5.14,5.16 (.8)	5.35,5.38 (.8)
L^p	5.00,5.01 (.2)	5.08,5.06 (.2)	5.14,5.09 (.1)	5.25,5.24 (.1)	5.48,5.48 (.1)	6.00,5.99 (.0)
Classic	5.00,5.02	5.02,5.03	5.03,5.04	5.07,5.08	5.14,5.16	5.32,5.34
Euclidean	5.00,5.01	5.01,5.02	5.02,5.03	5.06,5.07	5.13,5.15	5.29,5.31

(.) indicates the depth of the Median

It is observed from the above table that except similpicial depth, all the other depth represents the Euclidean median. The Oja procedures gives the results exactly as Euclidean procedure and it can tolerate upto 10% of contamination. When sample size increases the depth based on simplicial procedure doesn't provide the reliable result even though there is no contamination in the data. Halfspace and Projection procedures produces the results similar to Euclidean even when the sample sizes are increased.

4. Conclusion

Measure of location play a vital role in almost all statistical analyses. Now-a-days it is very difficult for the research community to find the exact measures in a data cloud due to heterogeneous, voluminous and huge dimensions of the data. This paper explores a number of depth based procedures and their properties are examined in order to find the measure namely median/centre. This paper

concludes that the Oja based depth procedure performed well by locating the median/centre in a data cloud and it can torelate upto certain level of contaminations. It works well in lower dimension but time consuming. Halfspace depth and projection depth gives the similar results. These procedures also satisfied the properties such as affine invariant, maximality at centre, monotonicity relative to the deepest point and vanishing at infinity. But, still it is a challenging task of the researcher to locate a centre point in a multi-dimensional data cloud.

References

1. Cascos, I. (2009). Data depth: Multivariate statistics and geometry (Kendall, W., and Molchanov, I., eds.) New Perspectives in Stochastic Geometry. Clarendon Press, Oxford University Press, Oxford.
2. Donoho, D. L., and Gasko, M. (1992). Breakdown properties of location estimates based on halfspace depth and projected outlyingness. Ann. Statist. 20, 1803–1827.
3. Liu, R.Y., Parelius, J.M., and Singh, K. (1999). Multivariate analysis by data depth: 2descriptive statistics, graphics and inference. The Annals of Statistics, 27, 783-858.
4. Liu, R. Y. (1990). On a notion of data depth based on random simplices. Annals of Statistics 18, 405–414.
5. Liu, R., and Singh. K. (1993). A quality index based on data depth and multivariate rank tests. Journal of the American Statistical Associaton, 88, 252-260.
6. Liu, R. Y., Serfling, R. and Souvaine, D. L., eds. (2006). Data Depth: Robust Multivariate Analysis, Computational Geometry and Applications. American Mathematical Society.
7. Mahalanobis, P.C. (1936). On the generalized distance is statistics. Proc. Nat. Acad. Sci. India, 12, 49-55.
8. Mosler, K. (2002). Multivariate Dispersion, Central Regions and Depth : The Lift Zonoid Approach. Springer, New York.
9. Mosler, K. (2013) Depth statistics (Becker C., Fried, R., Kuhnt, S., eds.) 17–34 Robustness and Complex Data Structures, Festschrift in Honour of Ursula Gather, Springer, Berlin,.
10. Oja, H. (1983). Descriptive statistics for multivariate distributions. Statistics and Probability Letter, 1, 327–332.
11. Rousseeuw, P. J., and Hubert, M. (1999). Regression depth (with discussion). J. Amer. Statist. Assoc. 94, 388–433.
12. Rousseeuw, P.J., Van Aelst, S., and Hubert, M. (1999). Rejoinder to the discussion of regression depth, Journal of the American Statistical Association, 94, 419-433.
13. Rousseeuw, P.J., and Leroy, A.M. (1987). Robust Regression and Outlier Detection, Wiley.
14. Serfling, R. (2006). Depth functions in nonparametric multivariate inference. In R. Liu, R. Serfling and D. Souvaine, eds., Data Depth: Robust Multivariate Analysis, Computational Geometry and Applications, 1–16. American Mathematical Society.
15. Small, C. G. (1990). A survey of multidimensional medians. Internat. Statist. Inst. Rev., 58, 263–277.

16. Tukey, J. W. (1975). Mathematics and picturing data. In Proceedings of the International Congress on Mathematics (R. D. James, ed.), 2, 523–531 Canadian Math. Congress.

17. Vardi, Y., and Zhang, C.-H. (1999). The multivariate L1-median and associated data depth. Preprint.

18. Yeh, A. B., and Singh, K. (1997). Balanced confidence regions based on Tukey's depth and the bootstrap. J. Roy. Statist. Soc. Ser. B 59, 639–652.

19. Weiszfeld, E. (1937). Tôhoku Math. J., 43, 355-386.

20. Wilcox, R.R. (2012). Introduction to Robust Estimation and Hypothesis Testing, Academic Press.

21. Zuo, Y., and Serfling, R. (2000). General notions of statistical depth function. The Annals of Statistics, 28, 461–482.

22. Zuo, Y. (2003). Projection-based depth functions and associated medians, The Annals of Statistics, 31, 1460-1490.

EFFECT OF ORGANIC MANURE IN CONTROLLING ENVIRONMENTAL POLLUTION

F.Jeyamangalam

Abstract

In the year 2010 a field experiment was conducted using theri soil at Poochikadu village which lies at 8°516' latitude and 78°052' longitude in Tuticorin district of Tamil Nadu, South India to evaluate the effect of different organic amendments and their combination on various physical properties on theri soil and their resultant impact on groundnut crop. The treatments of this study were farm yard manure (FYM), composted coir pith (CP) and tank silt (TS). The experiment was laid out in randomized block design with three replications. The yield of pods was high as 40.51% higher than control with the combination of CP and TS in equal combinations @ 12.5 t ha^{-1}. The bulk density (BD) and particle density (PD) has decreased in the plots. Percentage of water holding capacity (WHC), pore space (PS), saturated moisture (SM), hydraulic conductivity (HC) and permeability (PE) has increased. A holistic approach should be made by performing organic farming to reclaim theri soil without polluting the environment.

Keywords

Tank Silt, composted coir pith, amendment, reclamation, physical properties.

Introduction

The use of organic matter such as animal manures, human waste, food wastes, yard wastes, sewage sludges and composts has long been recognized in agriculture as beneficial for plant growth and yield and the maintenance of soil fertility. The new approaches to the use of organic amendments in farming have proven to be effective means of improving soil structure, enhancing soil fertility and increasing crop yields besides controlling environmental pollution. Organic matter is excellent source of plant-available nutrients and their addition to soil could maintain high microbial populations and activities.

Associate Professor, Department of Physics, Sarah Tucker College, Tirunelveli-627 007, Tamil Nadu, South India. E-mail: f.jeyamangalam@yahoo.com

Theri soils are made up of deep sand zones. The permeability of water is high; it faces higher level of soil erosion with low nutrients and minerals. Its water holding capacity is less, and is susceptible to wind erosion. Theri soils have a semi-arid tropical climate and therefore it is not suitable for agriculture. The Liberal addition of organic manures, silt and fertilizer in split doses and adequate liming are immediately needed to reduce the fertility constraints of theri soils (Jawahar *et al*., 1999).

The continued use of chemical fertilizers causes health and environmental hazards such as ground and surface water pollution by nitrate leaching (Pimentel, 1996). Positive effects of organic waste on soil structure, aggregate stability and water-holding capacity were reported in several studies (Odlare 2008). However, the low soil quality, such as the low hydraulic quality, high soil impedance, salt content and organic matter scarcity, limit the soil productivity seriously (Yao *et al*., 2009). Therefore, it is important to ameliorate the soil physical environment, decrease the salinity and increase soil nutrient for the soil quality improvement and the high efficiency without polluting soil by chemical fertilizers.

Materials and Methods

In the year 2010 field experiment was conducted at Poochikadu village which lies in $8^{o}516'$ latitude and $78^{o}052'$ longitude in Thuthukudi district of Tamil Nadu, South India. Groundnut (*Arachis Hypogea* L.) is grown best in sandy loam and loam soil as light soil helps in easy penetration of pegs, their development, and their harvesting. The variety chosen for cultivation was TMV-7 with duration of 105 days.

The disturbed soil samples were obtained using V shaped cut at the depth of 15 cms, air-dried ground, mixed, passed through 2 mm sieve and analyzed for their physico-chemical and physical properties. The experiment was laid down according to randomized block design. Groundnut crop was grown with proper weeding. Hand weeding was done at 20 and 40 days after sowing. The pod yield in each plot was measured.

Physical Properties

1. Bulk Density (BD)

Bulk density is defined as the mass (weight) per unit volume of a dry soil (volume of solid and pore spaces). It is also expressed in gm cm^{-3}. Bulk density normally decreases as mineral soils become finer in texture. Bulk density is of greater importance than particle density in understanding the physical behaviour of soils. Generally in normal soils bulk density ranges from 1 - 1.60 gm cm^{-3}.

2. Particle Density (PD)

The Weight per unit volume of the solid portion of soil is called particle density. It is also termed true density. It is expressed in gm cm^{-3}. Generally, in the normal soils the particle density is 2.65 gm cm^{-3}.

3. Maximum Water Holding Capacity (WHC)

Maximum water holding capacity is defined as the capacity of the soil to retain water is exceeded. At this point all soil pore spaces (micro and macro pore spaces) are filled up with water and the drainage is restricted.

4. Pore Space (PS)

Pore spaces (also called voids) in a soil consist of the portion of the soil volume not occupied by solids, either mineral or organic. The pore space under field conditions is occupied at all times by air and water. Pore spaces directly control the amount of water and air in the soil and indirectly influence the plant growth and crop production.

5. Saturated Moisture (SM)

At soil saturation, water fills completely in the pore spaces.

6. Hydraulic Conductivity (HC) and Permeability (PE)

The rate of flow of a liquid through a porous medium depends on the size, distribution and continuity of pores and the temperature of the fluid which is indexed as hydraulic conductivity. In case of soils saturated with water, it is directly related to permeability of the porous medium. The permeability of soil is calculated from the hydraulic conductivity.

The physical properties like PD, BD, WHC, HC, PE and PS were analyzed by Keen Raczkowski (KR) box given by Keen *et al.* (1921). HC and PE were analyzed using constant Head Permeater given by Israelsen and Hansen (1962). The data were statistically analyzed using analysis of variance (ANOVA) as applicable to complete the randomized block design, and least significant difference (LSD) at $P = 0.05$ was used to test the differences between means of individual treatments (Gomez and Gomez, 1984).

Results And Discussion

Physical Properties (After Harvest) - CP + (F+TS)

BD: The value of BD and PD had decreased in all plots than the control plot which is seen in

Physical Properties of Theri Soil for CP along with FYM & TS (After Harvest)

S.N	MANURE	PLOTS	BD	PD	WHC	PS	SM	HC	PE	YIELD
			gm/cm^3	gm/cm^3	%	%	%	cm/hr	mm / hr	Kg / ha
1	**CP**	T2-A1	1.5018 abc	2.4301 abc	24.6015	41.9909	27.4414	0.3003 e	2.9429 bcd	2698 e
2	**CP**	T2-B1	1.5194 abc	2.3930 abc	25.0772	38.3508	26.1673	0.3849 a	3.7720 ab	3065 bc
3	**CP**	T2-C1	1.4038 d	2.3100 d	27.8130	40.7145	28.4989	0.2621 cd	2.5686 d	2590 a
4	F+**CP**	T4-A1	1.5747 a	2.4849 abd	25.4954	40.3205	26.9811	0.3576 abc	3.5045 cd	2210 c
5	F+**CP**	T4-B1	1.5038 abc	2.4098 abc	26.7693	40.9108	28.3884	0.2539 de	2.4882 d	2945 d
6	F+**CP**	T4-C1	1.4571 bcd	2.2357 cd	25.3648	38.0804	27.5720	0.3795 ab	3.7191 ab	2123 a
7	**CP**+TS	T5-A1	1.5073 abc	2.4107 abd	24.3098	41.0945	24.5804	0.3276 abc	3.2105 abc	2620 de
8	**CP**+TS	T5-B1	1.5460 ab	2.4535 abd	27.0462	41.9697	28.2435	0.2867 bcd	2.8097 cd	3135 c
9	**CP**+TS	T5-C1	1.4893 abc	2.3605 abd	27.1422	40.8967	28.8711	0.2621 cd	2.5686 d	1895 a
10	F+**CP**+TS	T7-A1	1.4694 bcd	2.3414 bcd	26.0123	40.0173	28.6023	0.3658 ab	3.5848 abc	2935 e
11	F+**CP**+TS	T7-B1	1.4356 cd	2.4788 ab	26.2384	41.9950	27.0428	0.3945 a	3.8661 a	2868 ab
12	F+**CP**+TS	T7-C1	1.4092 d	2.2510 e	27.7421	38.4075	28.6727	0.4150 a	4.0670 a	1995 bc
13	Control	T81	1.5845 a	2.4981 a	23.0276	35.7437	23.5653	0.2530 de	2.4794 d	1865 de
	Grand Mean		1.4869	2.3931	25.6556	39.7805	26.9379	0.3138	3.1003	2534.2051
	Significance		**	*	NS	NS	NS	**	**	**
	SEd		0.0473	0.0680	3.9303	4.1108	3.7162	0.0462	0.4002	142.4305
	CD (P=0.05)		0.0977	0.1403	8.1118	8.4844	7.6699	0.0954	0.8259	293.9629
	CV %		3.90	3.48	18.76	12.66	16.90	18.04	15.81	6.88

NS – Not Significant * – Significant ** – More Significant
BD – Bulk Density PD – Particle Density WHC – Water Holding Capacity
PS – Pore Space SM – Saturated Moisture HC – Hydraulic Conductivity
PE – Permeability
F – Farm Yard Manure CP – Composted coir pith TS – Tank Silt
A – 7.5 t ha^{-1} B – 12.5 t ha^{-1} C – 17.5 t ha^{-1}

Table. The value of BD decreased as 1.5747, 1.5038 and 1.4571 gm cm^{-3} respectively in F+CP plot with organic manure @ 7.5, 12.5 and 17.5 t ha^{-1} respectively. Similar decrease in BD value was noted as 1.4694, 1.4356 and 1.4092 gm cm^{-3} in F+CP+TS amended plot @ 7.5, 12.5 and 17.5 t ha^{-1} respectively. The value of BD was lowest as 1.4038 gm cm^{-3} with CP manure @ 17.5 t ha^{-1}. It was 11.40% less than the control plot with value 1.5845 gm cm^{-3}. Here the BD values decreased to 1.4958 gm cm^{-3} @ 7.5 t ha^{-1} compared to control plot with 1.6014 gm cm^{-3} (Jeyamangalam *et al.*, 2011).

PD: The value of PD decreased as 2.4301, 2.3930 and 2.3100 gm cm^{-3} respectively with CP manure

plot @ 7.5, 12.5 and 17.5 t ha^{-1} respectively. The same trend was seen in F+CP plot as 2.4849, 2.4098 and 2.2357 gm cm^{-3} @ 7.5, 12.5 and 17.5 t ha^{-1} respectively. The minimum value was noticed in F+CP plot as 2.2357gm cm^{-3} @ 17.5 t ha^{-1} with the decrease of 10.50% than control plot with value 2.4981 gm cm^{-3}.

WHC: The water holding capacity was found to increase gradually as the dosage of organic manure increased. In the CP plot @ 7.5, 12.5 and 17.5 t ha^{-1} respectively WHC increased as 24.6015, 25.0772 and 27.8130% respectively. Similarly in CP+TS plots it increased as 24.3098, 27.0462 and 27.1422% and in F+CP+TS plots it increased as 26.0123, 26.2384 and 27.7421% @ 7.5, 12.5 and 17.5 t ha^{-1} respectively. The maximum value of WHC was noticed as 27.8130% in CP plot @ 17.5 t ha^{-1} which was 17.21% more than control plot with value 23.0276%. According to Saha *et al.,* (2010) the highest water holding capacity (54.67%) was also observed under continuous application of 100% NPK, FYM, bio fertilizer and lime.

PS: The pore space increased in all organic amended plots than control plot. The value of 41.9950% was noticed in F+CP+TS plot @ 12.5 t ha^{-1} with the increase of 14.89% than control plot having 35.7437%. The next higher value of PS was noticed in CP amended plot @ 7.5 t ha^{-1} with value 41.9909%. The value of PS ranged from 35.7437% to 41.9950%. Similar increase in pore space was reported by Jeyamangalam *et al.,* (2012) that soil total porosity varied from 35.74 to 45.39% in CP+(F+TS) combination before harvest was highest (45.39%) in CP plot @ 17.5 t ha^{-1}. The value was lowest as 35.55% in untreated control plot.

SM: In the present study, the value of SM increased in all plots than control plot. The value increased as 24.5804, 28.2435 and 28.8711% respectively in CP+TS plots @ 7.5, 12.5 and 17.5 t ha^{-1} respectively. The value was high as 28.8711% in CP+TS plot @ 17.5 t ha^{-1}. It was 18.38% higher than control plot with value 23.5653%. The major reason for the performance of maize plant was due to the effect of FYM on the organic matter and consequently moisture conservation. Earlier report of Shamsher Ali *et al.,* (2008) confirmed present findings.

HC: The hydraulic conductivity measurements provide an indication of relative water transmission rate of the soil. The value of HC increased in all plots than the control plot. The maximum value was 0.4150 cm hr^{-1} which was 39.04 % higher than control plot with value 0.2530 cm hr^{-1}. As the concentration of the organic manure increased, the HC values in F+CP+TS amended plot @ 7.5, 12.5 and 17.5 t ha^{-1} respectively increased with the value 0.3658, 0.3945 and 0.4150 cm hr^{-1} respectively. The WHC increased to 31.0583%, PS to 41.8819% and SM to 24.4252% respectively @ 12.5 t ha^{-1} against the control values 23.0276%, 35.7437% and 23.5653% in F+TS plot. The HC and PE values have also increased facilitating the available water supply to the plants (Jeyamangalam *et al*., 2014).

PE: The value of PE increased as 3.5848, 3.8661 and 4.0670 mm hr^{-1} respectively for F+CP+TS plot @ 7.5, 12.5 and 17.5 t ha^{-1} respectively. The control plot had the value of PE to be 2.4794 mm hr^{-1}. Malathesh (2005) explained that the farm yard manure seems to act directly by increasing crop yields either by acceleration of respiratory process by cell permeability or by hormone growth action. It supplies nitrogen, phosphorus and sulphur in available forms to the plants through biological decomposition. Indirectly, it improves physical properties of soil such as aggregation, aeration, permeability and water holding capacity. The present findings confirm this.

Yield – CP + (F+TS):

In the present study the maximum yield of groundnut was noticed as 3135 kg ha^{-1} with CP+TS plot @ 12.5 t ha^{-1}. It was 40.51% higher than the control as shown in Graph. Next higher yield of 39.15% was noticed for CP plot @ 12.5 t ha^{-1} with 3065 kg ha^{-1}. Saha *et al*., (2010) experienced a similar result as the FYM directly added an appreciable amount of major micronutrients to the soil, contribute to the enhanced yield.

Yield of Groundnut Pods using CP with F & TS (kg ha^{-1})

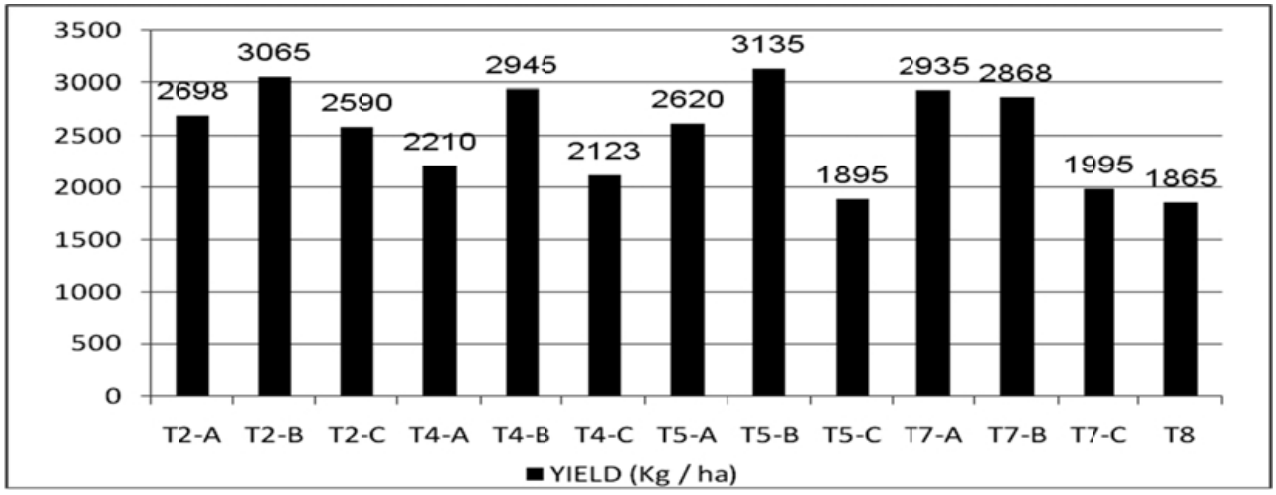

Plots containing different organic manure

Conclusion

Application of Composted coir pith provided positive effects on soil physical properties at different percentages. It can be said that CP is a soil conditioner with high water holding capacity. CP is a nutrient and Organic source which increases the yield. These results demonstrate the importance of the incorporation of CP to theri soil which is characterized by low organic matter content. It is recommended that CP+TS @ 12.5 t ha^{-1} can be added for improving soil properties since in the present study the yield was maximum as 3135kg ha^{-1} which is 40.51% higher than the control plot

with 1865 kg ha^{-1}. Organic manures provide all the essential nutrients required for growth and yield of the groundnut, with an added advantage of protecting the physico-chemical and physical characteristics of the soils by reducing the environmental pollution. Hence by organic farming the wind erosion and soil erosion are considerably decreased and paved the way for a healthy environment.

References

1. Gomez, K.A. and Gomez, A.A. 1984. *Statistical procedures for agricultural research*. New york: Wiley Inter Science, 2nd edn., P 95-109.
2. Israelsen, O.W. and Hansen, V.E. 1962. *Irrigation Principles and Practices* 3rd edn., John Wiley and Sons, Inc., New York.
3. Jawahar,D., Arunachalam,G., Velu,V and Ramaswami,P.P., 1999. Fertility capability of Theri-soils of Tamil Nadu. *Journal of Indian Society of Soil Science,* **47**(3): 570 – 573.
4. Jeyamangalam,F., Annadurai,B. and Arunachalam,N., 2011. Evaluation of organic amendments using FYM for the improvement of physical properties of Theri soil in Tamil Nadu, India. *Asian Science,* **6:** 35-40.
5. Jeyamangalam, F., Annadurai, B. and Arunachalam, N. 2012. Impact of composted coir pith and other organic sources on physico –chemical and physical properties and yield of groundnut. *J. Eco-Friendly Agriculture*, **7(1)**: 8-11.
6. Jeyamangalam,F., Annadurai,B. and Arunachalam,N., 2014. Effect of organic manuring on physical properties of Theri soil. *Journal of Eco-Friendly Agriculture*, **9(1):**16-20.
7. Keen, B.A**.** & Raczkowski, H. (1921). Relation between the clay content and certain physical properties of a soil. *Journal of Agricultural Science* **11**: 441-449.
8. Malathesh, G.H. 2005. Nutrient substitution through organics in maize. *M.Sc. (Agri.) thesis*, University of Agricultural Sciences, Dharwad.
9. Odlare,M., Pell,M and Svensson,K., 2008. Changes in soil chemical and microbiological properties during 4 years of application of various organic residues. *Waste Management Research*, **28**: 1246-1253.
10. Pimentel,D., 1996. Green Revolution and chemical hazards. *Science and Total Environment,* **188**: 86-98.
11. Saha, R., Mishra, V.K., Majumdar, B, Laxminarayana, K. and Ghosh, P.K. 2010. Effect of integrated nutrient management on soil physical properties and crop productivity under a maize (*zea mays*)-mustard (*Brassica campestris*) cropping sequence in acidic soils of northeast India. *Com.in Soil Science and Plant Analysis*, **41**:2187–2200.
12. Shamsher Ali Aman Ullah Bhatti, Abdul Ghani and Ahmad Khan. 2008. Effect of farmyard manure and inorganic fertilizers on the yield of maize in wheat-maize system on eroded inceptisols in Northern Pakistan. *14th Australian Agronomy Conference*.
13. Yao,R.J., Yang,J.S., Chen,X.B., Yu,S.P and Li,X.M., 2009. Fuzzy synthetic evaluation of soil quality in coastal reclamation region of North Jiangsu Province. *Scientia Agricultura Sinica*, **42**: 2019–2027. (in Chinese).

SOLAR ASSISTED PHOTOCATALYTIC DEGRADATION OF REACTIVE ORANGE 4 TO MINERAL ACID BY FLUORINATED TIO$_2$WACKHERR

A. Vijayabalan

Abstract

The photocatalytic decolourisation and degradation of an azo dye reactive orange 4 (RO4) in aqueous solution with F-TiO$_2$Wackherr as photocatalyst in slurry form have been investigated using solar light. F-TiO$_2$Wackherr is more efficient than TiO$_2$Wackherr in solar light. This catalyst was characterized by powder XRD, SEM, EDX. The effects of various parameters such as fluoride ion concentration, catalyst loading, pH, Initial concentration of the dye on degradation and decolourisation have been determined. The degradation was strongly enhanced in the presence of electron acceptor such as KIO$_4$. KBrO$_3$, H$_2$O$_2$, (NH$_4$)$_2$S$_2$O$_8$ and degradation is suppressed by Na$_2$CO$_3$, NaHCO$_3$

Keywords

TiO$_2$Wackherr; Solar light; Hydrofluoric acid; Reactive Orange 4;

1. Introduction

Recently, many efforts have been devoted to develop TiO_2 heterogeneous photocatalyst since it was approved to be a high efficient catalyst for environmental remediation and energy conversion purpose [1]. However, its technological application seems to be limited by several factors, among which the most restrictive one is the need for using an ultraviolet (UV), wavelength (l) <387 nm, as excitation source due to its wide band gap (3.2 eV for anatase) [2], and can only capture less than 5% of the solar irradiance at the Earth's surface. For the sake of efficient use of sunlight, or the use of the visible region of the spectrum, the technology of enlarging the absorption scope of TiO_2 may then appear as an appealing challenge for developing the future generation of photocatalysts. Several works reported that doping TiO_2 with nonmetallic elements, such as nitrogen, sulphur, carbon, shift the optical absorption edge of TiO_2 toward lower energy, thereby increasing the photocatalytic activity in visible region [3–5]. It was also demonstrated that F-doped TiO_2 is effective for enhancing photocatalytic activity. Yu et al. [6] proposed that F -doping converts Ti^{4+} to Ti^{3+} by charge compensation and the existence of Ti^{3+} can reduce the electron–hole recombination rate, and subsequently enhances

St.Joseph's College of Arts and Science (Autonomous), Manjakuppam, Cuddalore-1, Tamilnadu

the photocatalytic activity. Lin et al.(2005) reported that the Ag/F-TiO_2 samples show higher photocatalytic activities than that of F-TiO_2 sample under both UV and visible light irradiations[7], indicating that loaded Ag on F-TiO_2 is an effective way to improve photocatalytic activity. The strong interaction between the Ag nanoparticles and F-TiO_2 can effectively inhibit the recombination of excited electrons and holes and then enhance the photocatalytic performance. But, the excessive Ag particles can also act as recombination center and result in a decrease of photocatalytic activity. F-doping in TiO_2 can induce visible-light-driven photocatalysis by the creation of oxygen vacancies. However, the methods of preparing F-doped samples usually need special equipments or high temperature treatment. A few researchers have revealed that fluorination of TiO_2 powders in room temperature can improve photocatalytic activity [8–13]. Minero et.al. (2000) Claimed that surface fluorination of TiO_2 improves the photocatalytic oxidation rate of phenol and tetramethylammonium [10–12]; And they ascribed the phenomena to the enhanced generation of mobile free OH radicals. However, this surface fluorination calls for special pH range of the contaminated solution and that F^- ion are easy to run off in recycle reactions. Jingjing Xu, et al.(2008) reported that the fluorine-doped anatase titania solutions were synthesized by hydrolysis of titanium-n-butoxide in the presence of abundant acidic aqueous solution and using ammonium fluoride as fluorine precursors, under mild condition [14].

The Reactive Orange 4 (RO 4) dye (C.I. 18260, M. wt. 769.21) has been extensively used in dyeing the textile fabrics. The chemical structure of RO 4 is shown in Fig. 1. In our earlier work the degradation of toxic azo dye RO 4 using various photocatalysts was investigated [15-19]. In the present study, the solar photocatalytic degradation of RO4 using surface fluorinated TiO_2Wackherr is reported and the results are compared with UV light.

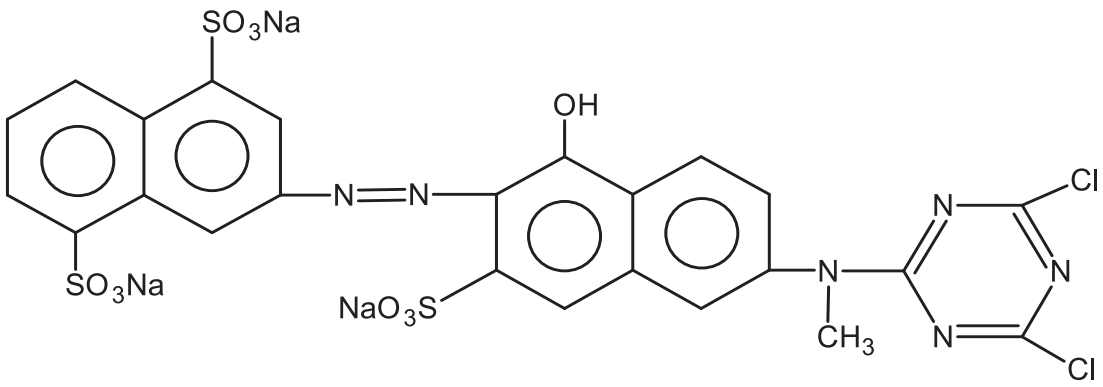

Fig. 1. Structure of Reactive Orange 4 dye

2. Materials

The studied pigment was Wackherr's ''Oxyde de titane standard'' (anatase), supplied by Sensient Cosmetic Technologies, F-95310, France. (Partical size of 300 nm and BET specific surface area of 8.5 m^2g^{-1}). Reactive Orange 4 (RO 4) (Colour Chem, Pondicherry) was used. AnalaR grade reagents H_2O_2 (30 w/w %), $(NH_4)_2S_2O_8$, $KBrO_3$, $KClO_3$, KIO_4, Na_2CO_3, Na_2SO_4, $NaHCO_3$ and $NaNO_3$ were obtained from Sd-fine and Merck company. The double distilled water was used to prepare experimental solutions. Hydrofluoric acid (HF) was used for fluorination. The natural pH of the aqueous solution is 4.8. The pH before irradiation was adjusted using H_2SO_4 or NaOH.

2.1. Experiment

2.1.1. Preparation of F-TiO_2 Wackherr

F-TiO_2 Wackherr was prepared by continuous stirring of the solution of appropriate amount of hydrofluoric acid and TiO_2 Wackherr for 3 hrs. F^- ions are able to displace OH groups on the surface of TiO_2 Wackherr quickly. F-TiO_2 was filtered, dried at 110°C for 2 hrs and used for degradation.

2.1.2. Irradiation experiments

All photocatalytic experiments were carried out under similar conditions on sunny days of April-May 2007 between 11 am to 2 pm An open borosilicate glass tube 50 mL capacity, 40 cm height and 20 mm diameter was used as the reaction vessel. The suspensions were magnetically stirred in the dark for 30 min to attain the adsorption- desorption equilibrium between the dye and F-TiO_2 Wackherr. Irradiation was carried out in the open air condition. For the experiments using the F-TiO_2-Wackherr, fluorination was achieved by adding appropriate concentration of hydrofluoric acid, corresponding to the required amount of F^- ion per gram of TiO_2 Wackherr. Fluoride ions are able to displace OH groups on the surface of TiO_2 very quickly [9]. The reaction mixture was continuously aerated by a pump to provide oxygen and for the complete mixing of the reaction solution. All the solutions prior to photolysis were kept in dark by covering with aluminum foil to prevent photochemical reactions.

2.1.3. Solar light intensity measurements

Solar light intensity was measured for every 30 min and the average light intensity over the duration of each experiment was calculated. The sensor was always set in the position of maximum intensity. The intensity of solar light was measured using LT Lutron LX-10/A Digital Lux meter and the intensity was 1250×100 lux. The intensity was nearly constant during the experiments.

2.1.4. Analytical method

In all the experiments 50 mL of reaction mixture was irradiated. At specific time intervals 1-2 mL of the sample was withdrawn and centrifuged to separate the catalyst. One milliliter of the sample was suitably diluted and its absorbances at 489 and 285 nm were measured immediately. Its absorbance at 489 nm (n- π* transition of –N=N– group) is due to the color of dye solutions and it is used to monitor the decolourization of dye. The absorbance at 285 nm ($\pi = \pi^*$ transition in naphthalene group) represents the aromatic content of RO 4 and the decrease at 285 nm indicates the degradation of aromatic part of dye. Since the decolourization is faster than degradation, the irradiation times of 10 min for decolourization and 30 min for degradation were chosen to compare the efficiencies. UV absorbance measurements were made using Hitachi U2001 Spectrophotometer. The pH of the solution was measured using HANNA Phep (Model H 198107) digital pH meter.

2.1.5. Photocatalyst Characterisation

Powder X-ray diffraction pattern Wackherr catalyst was obtained using a Philips PAN alytical X'pert PRO diffractometer equipped with a Cu tube for generating a CuKα radiation (wavelength 1.5406 Å) at 40 kV, 25 mA. The particles were spread on a glass slide specimen holder and the scattered intensity was measured between 20- 85° at a scanning rate of 2θ = 1.2°/min at 25 °C temperature. The digital output of the proportional X-ray detector and the goniometry angle measurements were sent to an online microcomputer for storing and analysis. Peak positions were compared with the standard JCPDS files to identify the crystalline phases. The crystalline size of TiO_2 Wackherr was determined using Debye-Scherrer equation (1).

$$D = \frac{K\lambda}{\beta \operatorname{Cos} \theta} \quad \ldots (1)$$

Where D is the crystal size of the catalyst, k is dimensionless constant, λ is the wavelength of X-ray, β is the full width at half-maximum (FWHM) of the diffraction peak and θ is the diffraction angle.

A Varian Cary 5E UV/VIS-NIR spectrophotometer equipped with an integrated sphere was used to record the diffuse reflectance spectra (DRS) and measure the absorbance data of the samples. The baseline correction was performed using a calibrated reference sample of barium sulfate. The reflectance spectra of the F-TiO_2Wackherr catalyst were analyzed under ambient conditions in the wavelength range of 200-800 nm

The morphologies of the oxides were determined using Hitachi, Model: S-3400N scanning electron microscope. Thermo Super Dry II Equipped with EDX was also used to record the energy dispersive X-ray spectrum.

3. Results and discussion

3.1. Crystal structure

Fig.2 shows the XRD patterns of bare TiO_2Wackherr (Fig.2a) and 0.48% fluorinated TiO_2Wackherr (Fig.2b) prepared with different concentrations of Fluoride ion. The pattern revealed that all the samples were composed of anatase phase matched with JCPDS Card No 89-4921 and average partical size was 88.0 nm. The fluorination had no obvious effects on the crystal structure of TiO_2Wackherr. Moreover, the doping F atoms did cause any shift in peak positions of TiO_2Wackherr. This could be understood that the ion radius of fluorine atom (0.133 nm) is virtually the same as the replaced oxygen atom (0.132 nm) [18].

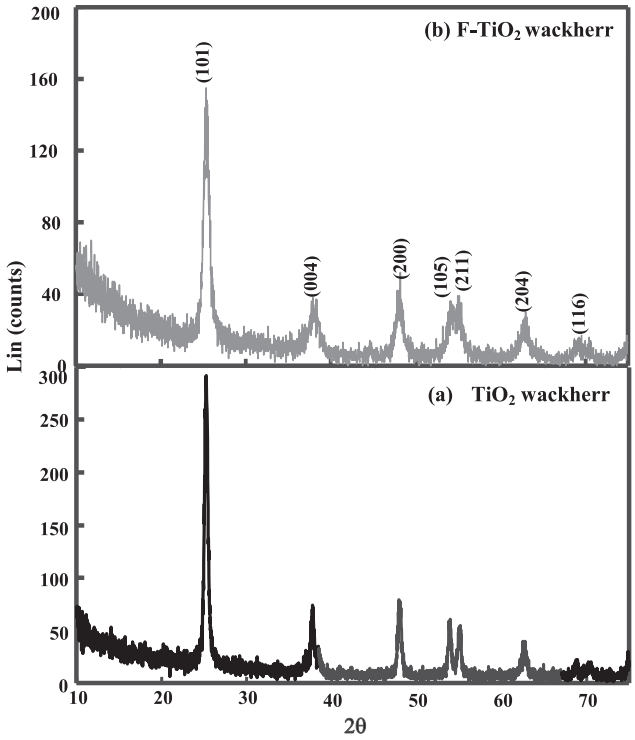

Fig.2. XRD of bare TiO_2Wackherr and F-TiO_2Wackherr

Optical properties

Diffuse reflectance spectroscopy gives information about the electronic absorption of the photocatalysts. Diffuse reflectance spectra of the TiO_2Wackherr and 0.48% F-TiO_2 Wackherr samples are shown in Fig.3a and 3b, respectively. Fluorination clearly influenced the light absorption characteristics. F-doping, absorption of TiO_2 was shifted to visible region. This conclusion is consistent with Asahi et al., Haneda et al., yamaki et al., and Ho et al. [20, 21, 22, and 23].

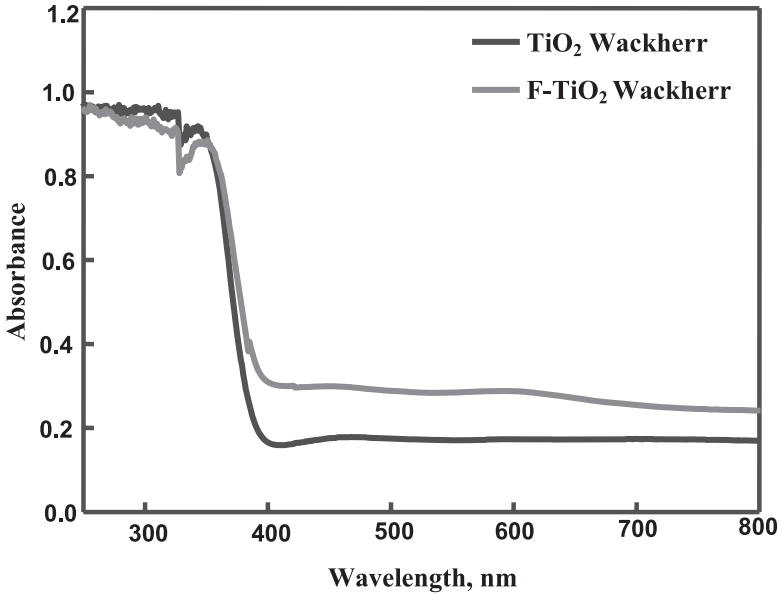

Fig.3.DRS of TiO_2Wackherr and F-TiO_2 Wackherr

Morphologies

The SEM images of TiO_2Wackherr and 0.48% F-TiO_2Wackherr are shown in Fig 4a and 4b, respectively. Both possessed spherical particle diameter of about in the range from 86 to 227 nm. The morphologies of the particles depend on the TiO_2 precursors as well as fluorine incorporation in TiO_2 matrix [24]. Energy dispersive spectrum was confirmed the F atom present in the surface of TiO_2Wackherr (Fig 5).

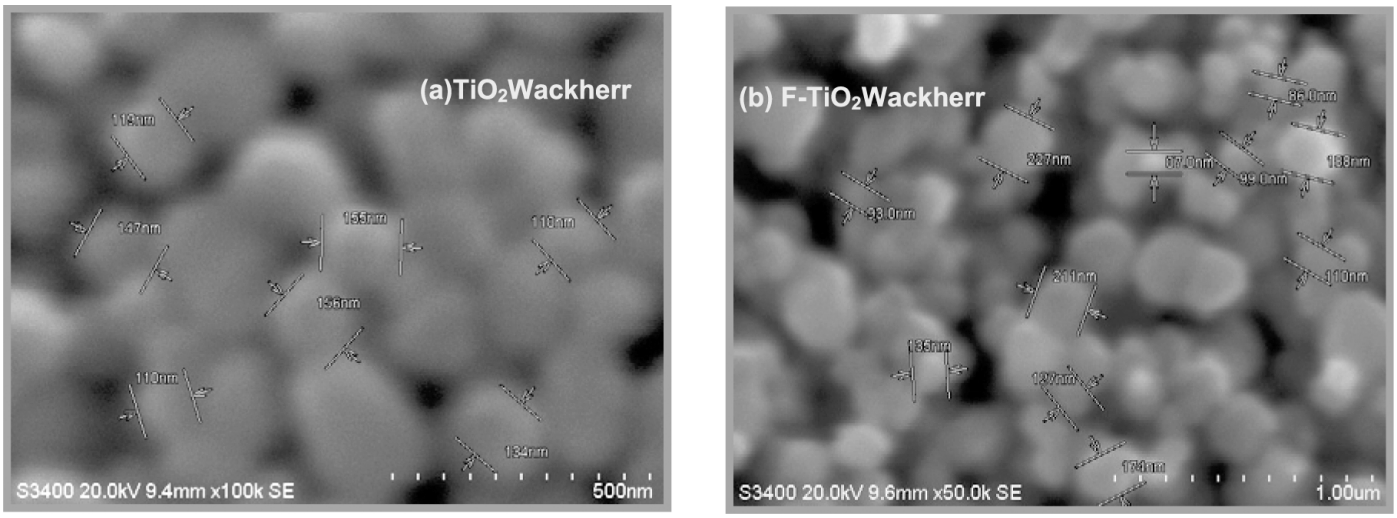

Fig. 4. SEM images of bare TiO_2Wackherr and F-TiO_2Wackherr.

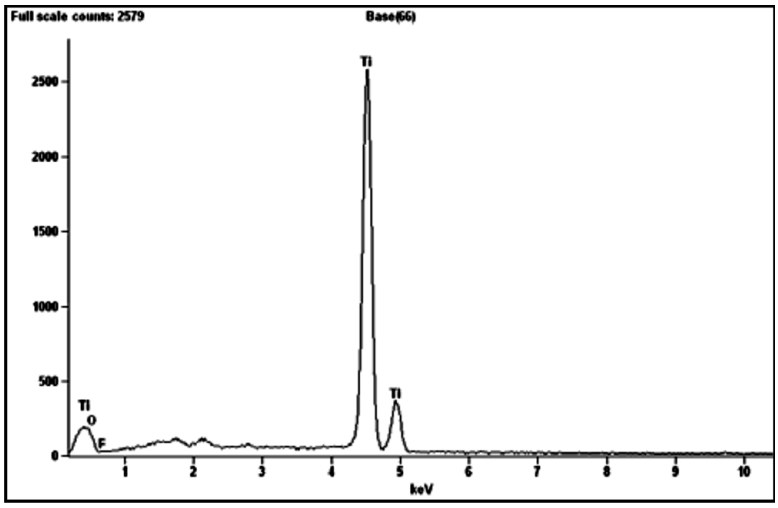

Fig. 5. EDS of F-TiO_2Wackherr

3.2. Effect of operational parameters

3.2.1. Photocatalytic activity study

Photocatalytic degradation of Reactive Orange 4 with bare TiO_2Wackherr and 0.48% fluorinated TiO_2Wackherr at pH 3 was investigated and the results are presented in Fig.6. It is observed that the RO4 degradation proceeded much more rapidly in the presence of F-TiO_2Wackherr. The 82 % degradation of RO4 was achieved at 60 minutes of irradiation with F-TiO_2Wackherr whereas only 60% degradation was occurred with bare TiO_2Wackherr under solar irradiation.

Vione *et al*. (2005) reported that the addition of fluoride to TiO_2 Wackherr in the pH range 2-5 induced an exchange with the hydroxyl groups on the surface of the photocatalyst [25]. …. (2)

$$Ti\text{-}OH + F^- \longleftrightarrow Ti\text{-}F + OH^-$$

The exchange is almost complete at pH 3.6-3.7. The Ti-F groups are not able to generate the surface species $^{\cdot}OH_{ads}$ but fluorinated Titania can induce the production of homogeneous $^{\cdot}OH$ in the bulk solution [11].

$$h^+_{vb} + H_2O_{ad} \rightarrow H_2O^{\bullet+} \text{ (on F-}TiO_2\text{-P25)} \quad \ldots (3)$$

$$H_2O^{\bullet+} \rightarrow H^+ + OH^{\bullet}_{free} \text{ (on F-}TiO_2\text{-P25)} \quad \ldots (4)$$

$$h^+_{vb} + Ti\text{-}OH_{surf} \rightarrow Ti\text{-}OH^{\bullet}_{surf} \text{ (on naked – } TiO_2\text{-P25)} \quad \ldots (5)$$

The photocatalytic degradation occurs mainly in solution phase by hydroxyl radicals. The oxidizing power of hydroxyl radicals produced by these catalysts is strong enough to break C-C, C-H, C=C bond of RO 4 leading to the formation of CO_2 and mineral acids. The formation of CO_2 was confirmed by the precipitation of $BaCO_3$, when the evolved gas during degradation was passed through concentrated $Ba(OH)_2$ solution.

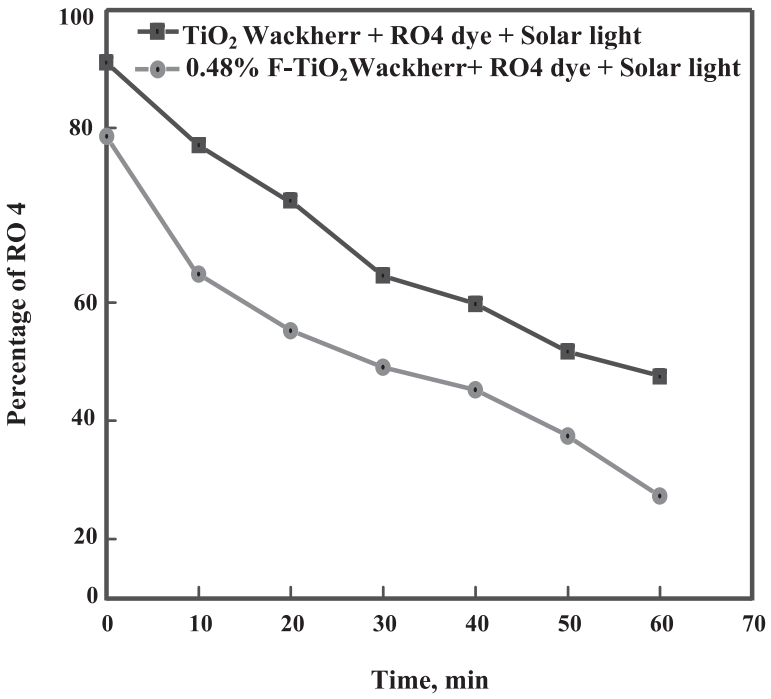

Fig.6. Photo degradability and adsorption of RO4; [RO 4] = 5×10^{-4} mol L^{-1}, pH = 3; Catalyst suspended : 0.48% F-TiO_2 Wackherr: airflow rate = 8.1 mL s^{-1}

3.2.2. Effect of fluorine content on TiO_2Wackherr

To investigate the optimum fluorine content on TiO_2Wackherr for efficient photo catalytic degradation, F-TiO_2 catalysts with 0.32 to 0.79 % fluorine content were prepared and tested for the degradation of RO4. The results are illustrated in Fig.7. It was found that rate constant for the degradation significantly increased from 0.024 to 0.031 min^{-1} with the increase of percentage of fluorine in TiO_2Wackherr from 0.32 to 0.48%. Further increase of F from 0.48 to0.79% decreased the rate constant from 0.031 to 0.019 min^{-1}. Hence under these experimental conditions 0.48% fluorinated TiO_2Wackherr was found to be optimum for efficient removal of RO 4 and may be due to that the interaction of fluoride ion with TiO_2 surface was maximized at 0.48% around pH=3. [10].

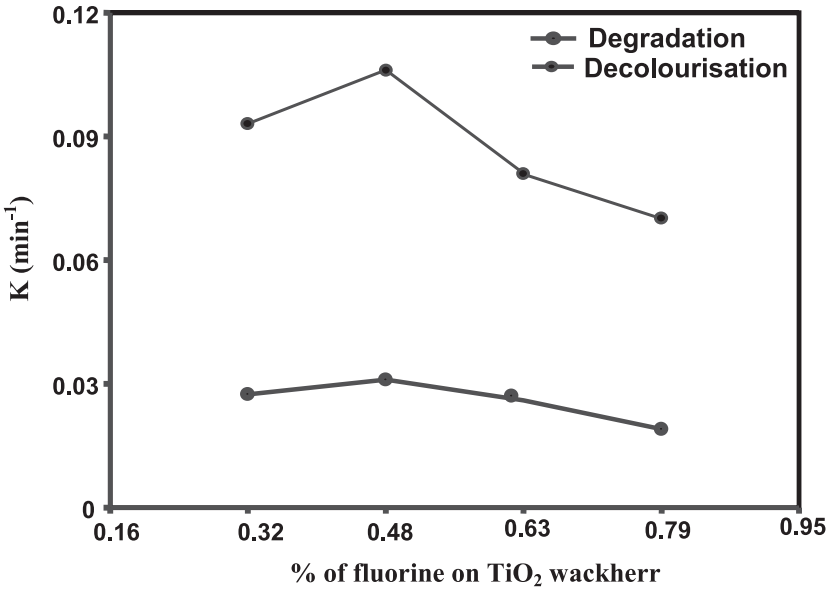

Fig.7. Effect of fluoride content on TiO_2Wackherr; [RO 4] = 5 × 10^{-4} mol L^{-1}, pH = 3 ; airflow rate = 8.1 mL s^{-1}.

3.2.3. Effects of catalyst loading:

Fig. 8 shows the effect of catalyst loading of F-TiO_2Wackherr on RO4 degradation at identical conditions. This figure shows the first order rate constants for different amounts of catalyst. The increase of F-TiO_2Wackherr from 6 to 10 g/L increasesed the rate constant from 0.009 to 0.031 min^{-1}. Further increase of catalyst

amount from 10 to 12 g/L decreased rate constant from 0.031 to 0.018 min^{-1}. Hence the optimum dosage of F-TiO_2Wackherr was 10 g/L. Due to the low scattering of UV radiation by F-TiO_2Wackherr, the degradation rate of RO4 dye continued to increase with increasing photocatalyst loading upto 10g/L. The decrease in degradation rate from 10 to 12g/L, due to high scattering of radiation by TiO_2Wackherr at higher concentration. It was reported that UV radiation scattering by TiO_2 Degussa P25 was higher than scattering by TiO_2 Wackherr [22] or [24].

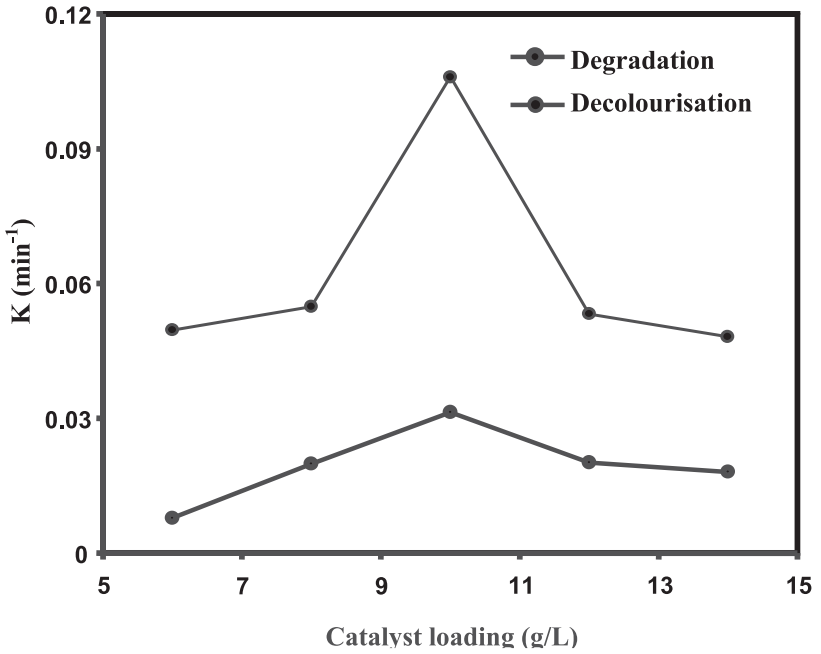

Fig.8. Effect of Catalyst amount; [RO 4] = 5 × 10^{-4} mol L^{-1}, pH = 3; airflow rate = 8.1 mL s^{-1}

3.2.4. Effect of solution pH

In order to find the optimum pH on the photocatalytic degradation of RO 4 by F-TiO_2 Wackherr, photocatalytic degradation of RO 4 on the catalyst was performed at different pH values and the results are presented in Fig 9. The degradation rate constants of RO 4 were 0.009, 0.031, 0.011, 0.010 and 0.009 min^{-1} at pH 1, 3, 5, 7 and 9 respectively. The same trend was observed with decolourisation rate constants. Hence pH 3 was recorded to be optimum for efficient dye removal.

An experiment on the dark adsorption of RO 4 under different pH was carried out. The percentages of adsorption at pH 3, 6 and 9 were found be 23, 20 and 10 at the time of 30 min. Ti-FH^+ may exist in the place of $TiOH_2^+$ at pH3 and this may lead to the strong

adsorption of dye at this pH. The highest degradation rate at pH 3 indicated that the adsorption of RO 4 played a vital role in the degradation mechanism.

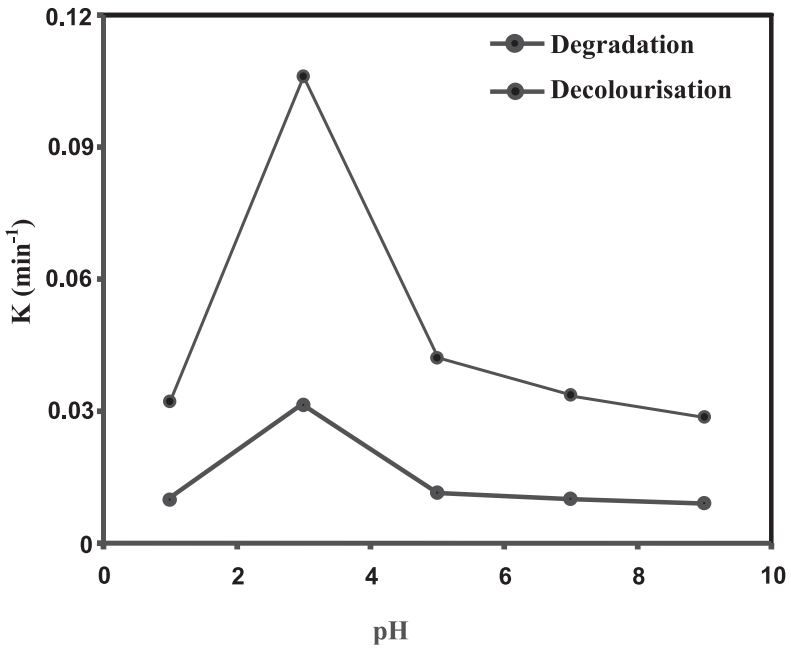

Fig.9. Effect of solution pH; Catalyst suspended=0.48% F-TiO_2 Wackherr, [RO 4] = 5×10^{-4} mol L^{-1}, airflow rate = 8.1 mL s^{-1}.

3.2.5. Effect of substrate concentration

The effect of the initial RO4 concentration on its degradation with F-TiO_2 Wackherr was investigated by varying dye concentrations from 3 to 7×10^{-4} mol/L at pH 3 and the results are given in Fig. 10. Table 1. shows that the increase of initial dye concentration from 3 to 7×10^{-4} mol/L decreases the percentage of degradation both in TiO_2Wackherr and F-TiO_2Wackherr. It was found that even at 7×10^{-4} mol/L concentration of RO4 about 40% dye removal could be achieved by F-TiO_2Wackherr. The decrease of degradation efficiency with increase of dye concentration of RO4 was due to low penetration of light.

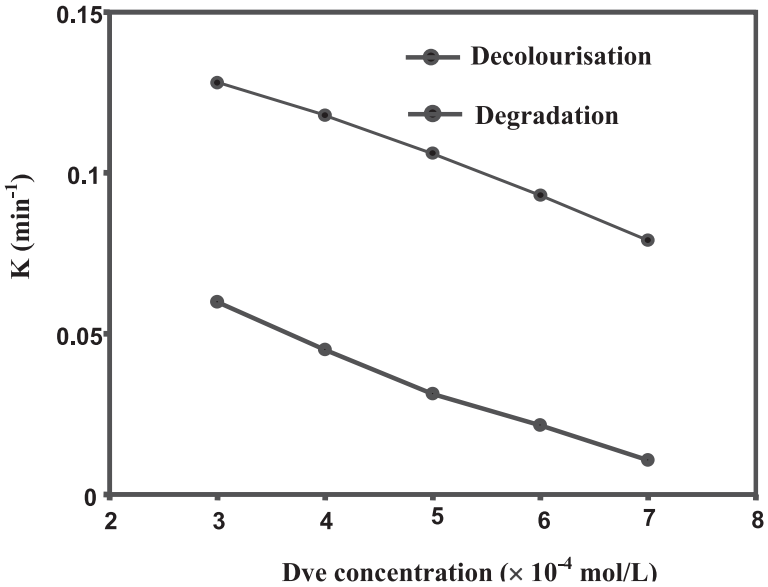

Fig.10. Effect of various initial dye concentrations; Catalyst suspended=0.48% F-TiO_2 Wackherr, [RO4] = 5x10^{-4} mol L^{-1}, pH = 3; airflow rate = 8.1 mL s^{-1}.

Table 1
The degradation of various initial dye concentrations of RO4 by F-TiO_2 Wackherr and bare TiO_2 Wackherr

Dye concentrations (×10^{-4}M)	Reactive Orange 4 Degradation (%)	
	TiO_2Wackherr	0.48% F-TiO_2Wackherr
3	52.47	69.31
4	49.32	65.26
5	45.34	60.90
6	39.08	56.62
7	35.58	49.66

3.2.6. Other factors influencing photodegradation of RO 4 with F-TiO_2wackherr

The influence of various oxidants on degradation of RO 4 with 0.48% F-TiO_2Wackherr was examined with optimized condition [(RO 4) = 5 × 10^{-4} mol/L; airflow rate = 8.1 mL^{-1} s^{-1}; pH = 3]. (Table 2) Addition of oxidants such as KIO_4, $(NH_4)_2S_2O_8$, $KClO_3$, $KBrO_3$ and H_2O_2 enhanced the photodegradation of RO 4. The higher degree of degradation in this process with the oxidants was due to formation of highly reactive radical intermediates and the electron capture by these oxidants (eqns. 6-13).

$IO_4^{\bullet-} + h\nu \rightarrow IO_3^{\bullet} + O^{\bullet-}$ … (6)

$O^{\bullet-} + H^+ \rightarrow {}^{\bullet}OH$ … (7)

$H_2O_2 \xrightarrow{h\nu} {}^{\bullet}OH$ … (8)

$S_2O_8^{2-} \xrightarrow{h\nu} 2SO_4^{\bullet-}$ … (9)

$SO_4^{\bullet-} + H_2O \rightarrow {}^{\bullet}OH + SO_4^{2-} + H^+$ … (10)

$S_2O_8^{2-} + e_{CB}^- \rightarrow SO_4^{\bullet-} + SO_4^{2-}$ … (11)

$BrO_3^- + 6\, e_{CB}^- + 6H^+ \rightarrow Br^- + 3H_2O$ … (12)

$ClO_3^- + 6\, e_{CB}^- + 6H^+ \rightarrow ClO_2^- + H_2O_2$ … (13)

Table 3 gives the percentage degradation on the addition of inorganic anions like carbonate, bicarbonate, sulfate and nitrate at pH 3. All the anions decreased the degradation and decolourisation rate constants. This decrease may be due to hydroxyl radical quenching effect by inorganic anions.

Table 2. Effect of oxidants on photodegradation of RO 4 with F-TiO_2Wackherr

Oxidants	Degradation (%)	Decolourisation (%)
0.48% F-TiO_2Wackherr	60.90	65.36
KIO_4	88.75	98.08
$KBrO_3$	84.50	92.60
$(NH_4)_2S_2O_8$	64.70	70.35
$KClO_3$	67.82	78.20
H_2O_2	85.47	94.16

Table. 3 Effect of inorganic anions on photodegradation of RO 4 with F-TiO_2Wackherr and TiO_2 Wackherr

Anions	Degradation (%)	Decolourisation (%)
0.48% F-TiO_2 Wackherr	60.90	65.36
$NaNO_3$	41.34	52.74
Na_2SO_4	79.10	85.06
$NaHCO_3$	35.20	44.43
Na_2CO_3	21.77	36.65

3.2.7. Effect of Oxidation of I^- ion by F-TiO_2Wackherr

To find out the mechanism of highly efficient photodegradation of F-TiO_2Wackherr, iodide ion oxidation experiments were carried out by TiO_2Wackherr phototcatalysis with and without surface fluorination (Fig.11). It is well known that I^- ion is very easily oxidized by the holes formed from excited TiO_2Wackherr to produce I_2. Therefore, the yield of holes can be determined by estimating the produced I_2. Irradiation of 0.1 M of KI with TiO_2Wackherr and F-TiO_2Wackherr under the same conditions, with solar light for 60 min shows higher iodine generation for F-TiO_2Wackherr. The iodine formed was found from the absorbance spectra of the illuminated solutions. This iodide ion oxidation revealed that the concentration of iodine formed in the presence of F-TiO_2Wackherr was up to three a time of that was in the presence of bare TiO_2Wackherr.

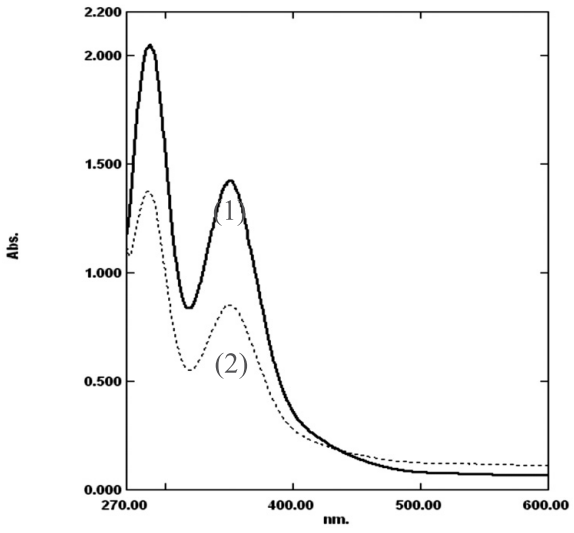

Fig. 11. Oxidation of I^- ion in aqueous suspension with 1. F-TiO_2Wackherr 2. TiO_2Wackherr

Fig. 11. Oxidation of I^- ion in aqueous suspension with 1. F-TiO_2Wackherr 2. TiO_2Wackherr

3.2.8. The comparison of degradation of RO4 dye by F-TiO_2Wackherr under UV and Solar process

Table 4. reveals that the degradation of RO4 dye by UV-F-TiO_2Wackherr is much faster than solar-F-TiO_2Wackherr, UV-TiO_2Wackherr and solar-TiO_2Wackherr respectively.

Table. 4.
The comparison of degradation of RO4 dye by F-TiO_2 Wackherr under UV and Solar process

Process	degradation (%)	decolourisation (%)
UV/TiO_2Wackherr	50.17	61.20
Solar/TiO_2Wackherr	45.34	54.86
UV/F-TiO_2Wackherr	65.20	74.56
Solar/F-TiO_2Wackherr	60.90	65.36

4. Conclusion

F-TiO_2Wackherr had higher absorption in the UV region of solar light than TiO_2 Wackherr. Degradation of RO4 with F-TiO_2Wackherr was faster than TiO_2Wackherr under artificial solar light. The high photocatalytic activity of F-TiO_2Wackherr may due to extrinsic absorption through the creation of oxygen vacancies rather than the excitation of the intrinsic absorption band of bulk TiO_2. This catalyst is suitable for treatment of dye effluent at higher dye concentration. Optimum pH and catalyst loading for higher efficiency are 3 and 10gL^{-1} respectively. Addition of oxidants increased the degradation rate whereas addition of inorganic anions decreased the degradation rate. Without any special treatments, F-TiO_2Wackherr can be applied to recycle use in photocatalytic reactions while keeping high activity.

References

1. J.T. Chang, Y.F. Lai, J.L. He, Surf. Coat. Technol. 200 (2005) 1640.
2. T. Yang, M. Yang, C. Shiu, W. Chang, M. Wong, Appl. Surf. Sci. 252 (2006) 3729.
3. R. Asahi, T. Morikawa, T. Ohwaki, Science 293 (2001) 269.
4. J.C. Yu, W. Ho, J.G. Yu, H. Yip, P.K. Wong, J.C. Zhao, Environ. Sci. Technol. 39 (2005) 1175.
5. S.U.M. Khan, M. Al-shahry, W.B.Jr. Ingler, Science 297 (2002) 2243.
6. J.C. Yu, J.G. Yu,W.K. Ho, Z.T. Jiang, L.Z. Zhang, Chem. Mater. 14 (2002) 3808.
7. D. Li, H. Haneda, N.K. Labhsetwar, S. Hishita, N. Ohashi, Chem. Phys. Lett. 401 (2005) 579.
8. A. Hattori, K. Shimota, H. Tada, S. Ito, Langmuir 15 (1999) 5422.
9. C.M. Wang, T.E. Mallouk, J. Am. Chem. Soc. 112 (1990) 2016.
10. C. Minero, G. Mariella, V. Maurino, E. Pelizzatti, Langmuir 16 (2000) 2632.
11. C. Minero, G. Mariella, V. Maurino, D. Vione, E. Pelizzetti, Langmuir 16 (2000) 8964.
12. M.S. Vohra, S. Kim, W. Choi, J. Photochem. Photobiol. A 160 (2003) 55.
13. A. Hattori, M. Yamamoto, H. Tada, S. Ito, Chem. Lett. 8 (1998) 707
14. Jingjing Xu, Yanhui Ao, Degang Fu, Chunwei Yuan, Journal of Physics and Chemistry of Solids 69 (2008) 2366– 2370
15. Muruganandham M, Swaminathan M. Solar photocatalytic degradation of a reactive azo dye in TiO_2 suspension. Solar Energy Materials and Solar Cells 2004;81:439-457.
16. Muruganandham M, Swaminathan M. Photochemical oxidation of reactive azo dye with UV-H_2O_2 process. Dyes and Pigments 2004; 62:269-275.
17. Muruganandham M, Swaminathan M. Decolourisation of Reactive Orange 4 by Fenton and photo-Fenton oxidation technology. Dyes and Pigments 2004; 63:315-321.
18. Chu W. Modeling the quantum yields of herbicide 2, 4-D decay in UV/H_2O_2 process. Chemosphere 2001; 44:935-941.
19. Alaton IA, Balcioglu IA, Bahnemann DW. Advanced oxidation of a reactive dye bath effluent: Comparison of O_3, H_2O_2/UV-C and TiO_2/UV-A processes. Water Research 2002; 36:1143-1154.
20. R. Asahi, T. Morikawa, T. Ohwaki, Science 293 (2001) 269.
21. D. Li, H. Haneda, S. Hishita, N. Ohashi, N.K. Labhsetwar, J. Fluorine Chem. 126 (2005) 69.
22. T. Yamaki, T. Umebayashi, T. Sumita, S. Yamamoto, M. Maekawa, A. Kawasuso, H. Itoh, Nucl. Instrum. Methods Phys. Res. B 306 (2003) 254.
23. W. Ho, J.C. Yu, S. Lee, Chem. Commun. (2006) 1115.
24. Xu. J, AO. Y, Fu .D, Yuan . C, Low-temperature Preparation of F-doped TiO_2 film and its Photo catalytic activity under Solar light, Applied Surface Science 254 (2008) 3033-3038.
25. D.Vione, C.Minero, V.Maurino, E.Carlotti, T.Picatonotto, E.Pelizzetti. Appl. Catal.B: Environ. 58 (2005) 79-88.

A HIGH-AVAILABILITY AND INTEGRITY OF DATA FOR CLOUD STORAGE IN CLOUD COMPUTING

[1]C. Rajalakshmi [2]Dr.M.Germanus Alex [1]G. Santhana Devi [1]
V.P.Kulalvaimozhi [1]M. Muthulakshmi [1]R. Mariselvi

Abstract

Cloud computing has recently raised an important attention worldwide. There exist several different definitions of cloud computing. Gartner defines cloud computing as "a style of computing where massively scalable IT-enabled capabilities are delivered 'as a service' to external customers using Internet technologies". According to NIST, National Institute of Standards and Technology, Cloud Computing is "a model for enabling convenient, on-demand network access to a shared pool of configurable computing resources (e.g., networks, servers, storage, applications, and services) that can be rapidly provisioned and released with minimal management effort or service provider interaction". Despite many different existing cloud definitions, both Gartner and NIST agree the cloud paradigm aims at offering every network-accessible computing resource "as-a-Service". The aim of this paper is to present the current state of security in the cloud computing, and highlight possible security issues and vulnerabilities associated with ' cloud infrastructures. Research is based on an overview of existing literature and personal experience gained in analysis of different cloud platforms and applications.

Keywords

Cloud Computing, Computer Security, Network, Service models.

1. Introduction

1.1 Cloud Computing

Cloud computing is largely a combination of existing and known technologies that were available in the early 1990s (grid computing, utility computing and virtualization). Each of these technologies form a component in the layers of cloud computing, which allow the user to pay only for

[1] *Prof Department of Computer Science, Kamarajar Government Arts College, Surandai.*

[2]*Prof & Head of the Department of Computer science, Kamarajar Government Arts College, Surandai. Corresponding Author : rajiamdr@gmail.com*

the resources used rather than paying a fixed price. This revolutionary model has enabled various companies and organizations in need of additional resources to purchase additional computing power without having to put forth a large capital investment in their proprietary IT-infrastructure. One of the main factors that came into cloud computing is virtualization technology which allows the resource usage to be dynamically sized (decreased or increased on demand).

Even though cloud computing brings many benefits and reduces costs, there is still much distrust of such services from a security standpoint, and a lot of security concerns. Before moving to the cloud, organizations must have a well-defined methodology. Data migration is more than just transferring data from one system to another. To prepare and excute a successful data migration there needs to be a well-defined medhodology for data migration. Cloud computing should be approached carefully and the data sensitivity should be taken in consideration. By adopting the cloud model, organization doesn't have the control over their data, which a more classical model provides. By doing so, they trust the provider's security policy. Security and privacy issues must be addressed at an early stage, because the subsequent changes could bring many complications, which can be expensive and risky.

1.2 Characteristics

Cloud computing is a model for enabling convenient, on demand network access to a shared pool of configurable computing resources that can be rapidly provisioned and released with a minimal management effort or service provider interaction. For a more accurate definition of cloud, there are essential characteristics presented, starting with an on-demand self-service where a customer may increase or decrease the amount of desirable computing resources automatically without any human interaction with each service provider. Broad network access enables access to the computer resources over the network using standard mechanisms. With resource pooling provider's resources are shared between numerous customers.

1.3 Deployment Models

Depending on infrastructure ownership, three major types of cloud deployments are known: public clouds, private clouds and hybrid clouds. Every model has its own pros and cons. Fig. 1.1 presents an example of how applications in hybrid cloud can be run in public cloud while sensitive information is stored in private cloud.

Public cloud is the model in which services and facilities are available through the Internet, using web applications, from an off-site third-party provider who shares resources and bills on a fine-grained utility computing basis. It can be owned, operated and managed by business, academic or

government organizations, or even some combinations' of all. Such clouds have the highest level of efficiency in sharing resources, but are also more vulnerable than private clouds.

Private cloud is designed exclusively for a specific organization, which includes more consumers (business units). Private cloud can be hosted in a data center or any other business locations (local housing). Cloud services may be performed by the organization itself or a third party.

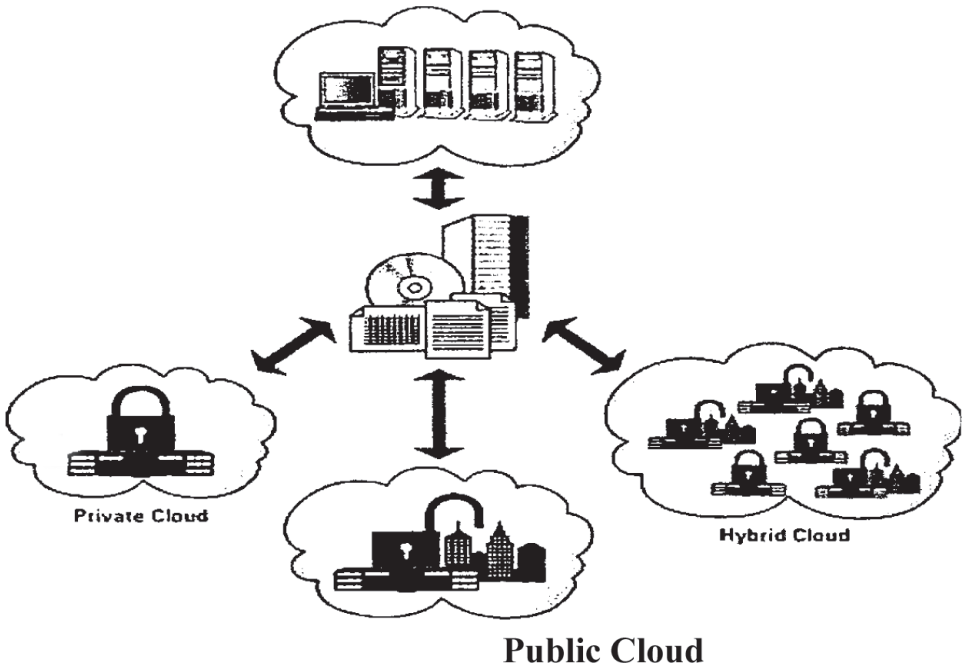

Fig. 1.1 Three major types of cloud deployment

Hybrid cloud is composed of two or more different cloud infrastructures (private/public or virtual/actual) as shown on Fig. 1.3. The model keeps running separate entities which a,re linked together using standard techniques such as standardized APIs, which provide an easier communication and the distribution of roles in different models of clouds.

1.4 Service Models

Service models represent the different delivery models that are in use with a particular deployment model. These delivery models are the SaaS (Software as a Service), PaaS (Platform as a Service) and IaaS (Infrastructure as a Service).

1.4.1 Software as a Service (SaaS)

The purpose of the service is to provide the consumer with the use of provider's applications running on a cloud infrastructure. Applications are available on different devices and clients (web e-mail). The customer does not manage the provider's cloud or control the basic infrastructure (cloud

network, servers, operating systems, storage, applications, settings, etc.).

1.4.2 Platform as a Service (PaaS)

PaaS has several advantages for developers. Platform as a Service is a way to rent hardware,

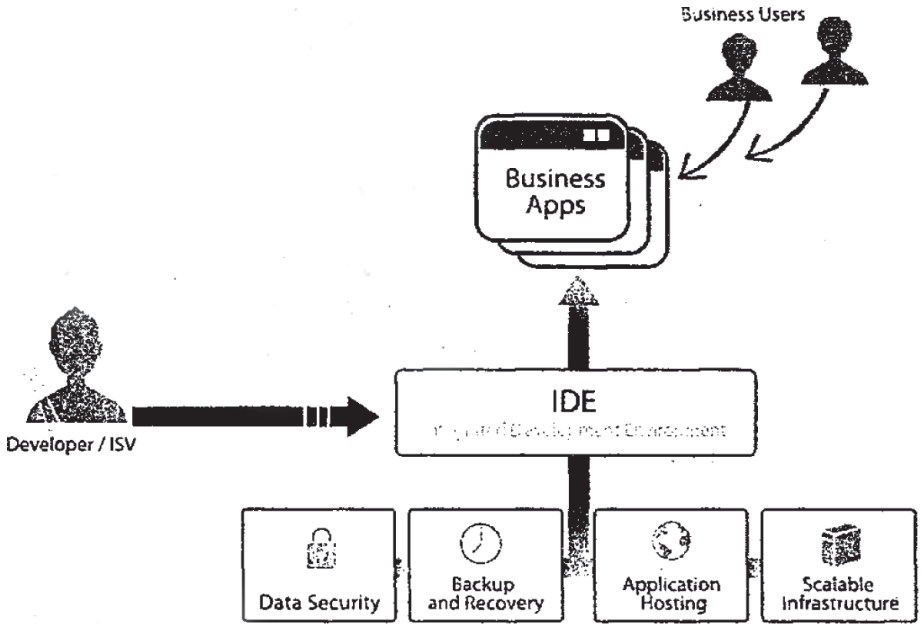

Fig. 1.2 Developer using Platform as a Service

on which cloud customers are able to develop and implement applications that are developed in programming languages and tools supported by the cloud provider as shown below in Fig. 1.2.

Client has no control over the basic infrastructure, but has the control over the applications and settings used for the application environment. The primary purpose of the service is to reduce the cost and complexity of purchasing, hosting and managing hardware and software for running the company's applications. The development environment is usually dedicated and determined by the cloud provider and is in accordance with the platform. The responsibility of security is shared between the provider and the company which makes the use of the cloud.

1.4.3 Infrastructure as a Service (IaaS)

IaaS is the most basic model of cloud services. The consumer can implement any software, including operating system and applications. Client has a considerable freedom to choose the operating system, and while he doesn't control or manage the basic infrastructure, he can control the operating

system, applications, and in some cases even a basic firewall. The primary purpose of the service is to avoid the purchase, maintenance and hosting of hardware and software resources.

1.5 Cloud Computing Security Issues

Cloud computing constitutes a new technology when it comes to data hosting by external companies it is an interesting, economic model, that induces security concerns. Most security issues in cloud services are not new, as there have been pre-existing hosting services for many years, that offered accounts on shared servers or common hardware. Today there are several established organizations which are involved primarily in security in the cloud. Among these organizations is CSA (Cloud Security Alliance) at the forefront, which has, in the end of the year 2009, issued a document, entitled «Security Guidance for Critical Areas and Cloud Computing)). CSA is a non-profit organization formed in late 2008. The founding members are mainly industry representatives and many corporate members such as Google, Microsoft, IBM, and VMware.

Jim Reavis, founder and executive director of the Cloud Security Alliance stated that "enterprises across sectors are eager to adopt cloud computing - but that security standards are needed both to accelerate cloud adoption on a wide scale and to respond to regulatory drivers".

Different organizations would need to examine the security and confidentiality concerns using cloud computing as a service for their business critical insensitive applications. However, the security of business data in the cloud is difficult to achieve or sometimes even impossible. SaaS, PaaS and IaaS all expose their own security concerns.

1.5.1 Data protection

When it comes to data gathering, companies which decide to outsource their data to cloud providers do it willingly, knowing in a measure the resources they use are shared with other Cloud provider's customers. It is important to improve reliability: Storing data on cloud is an effective way to improve the reliability, knowing the data and applications are stored and backed up on several computers, making the chances of data and application loss reduced.

Special cases of data protection are databases. Some cloud environments allow multiple instances where the user has its own database and can control access to the database and set him the rights permissions. Most of these cases can preserve data integrity. The second model assumes the customer has a predefined environment shared with other users. By using a central global transaction manager, it is possible to keep the data in a system where transactions are made from multiple data sources.

1.5.2 Privacy

Most of the cloud providers make clear statements when it comes to privacy. Google Apps has five privacy principles which explain how it engages its responsibility when it comes to data privacy. However not all cloud providers have the same clear statements. Some other services, such as Drop box (a SAAS which makes the data sharing easier), clearly state it is possible for the company to use, alter and diffuse users' data.

The only thing companies could be sure about is that their cloud provider has to expose and present their data-privacy policy more than the offer, companies would carefully read the policy terms and make sure it is clear when it comes to privacy. Cloud providers must be vigilant when it comes to privacy, because it should be a fundamental objective throughout the planning of a cloud, which has to cover both provider services and end-users.

1.5.3 Cryptography

The current threat comes from the servers involved in the cryptographic algorithms. Random bytes being generated present poor entropy, making the job easier for hackers. Organizations which decide to move sensitive data in the cloud must therefore choose the way how encryption is controlled and the data safely stored. The data stored in the cloud could have different natures (eg, records that the user creates or use, applications, information, configurations, development tools, etc.). To protect data from any unauthorized access, the most commonly used measures are encryption and access control. A special care is required about reading privacy-sensitive information.

2. Literature Review

In [1] Ateniese G., et al. (2007) proposed a model for provable data possession (PDP) that allows a client that has stored data at an untrusted server to verify that the server possesses the original data without retrieving it. Thus, the PDP model for remote data checking supports large data sets in widely-distributed storage systems. We present two provably-secure PDP schemes that are more efficient than previous solutions, even when compared with schemes that achieve weaker guarantees. In particular, the overhead at the server is low (or even constant), as opposed to linear in the size of the data.

In [2] Ateniese G., et al. (2008) proposed that a storage outsourcing is a rising trend which prompts a number of. interesting security issues, many of which have been extensively investigated in the past. However, Provable Data Possession (PDP) is a topic that has only recently appeared in the research literature. The main issue is how to frequently, efficiently and securely verify that a storage

server is faithfully storing its client's (potentially very large) outsourced data.

In [3] Bellare M., et al. (1994) proposed to initiating the investigation of a new kind of efficiency for cryptographic transformations. The idea is that having once applied the transformation to some document M, the time to update the result upon medication of M should be proportional to the amount of modification done to M.

In [4] Bowers K.D., et al. (2009) proposed a distributed cryptographic system that allows a set of servers to prove to a client that a stored file is intact and retrievable. HAIL strengthens, formally unifies, and streamlines distinct approaches from the cryptographic and distributed-systems communities.

In [5] Bowers K.D., et al. (2009) proposed a compact proof by a file system (approver) to a client (verifier) that a target file F is intact, in the sense that the client can fully recover it. As PORs incur lower communication complexity than transmission of F itself, they are an attractive building block for high-assurance remote storage systems. It proposes a theoretical framework for the design of PORs. The framework improves the previously proposed POR constructions of Juels-Kaliski and Shacham-Waters, and also sheds light on the conceptual limitations of previous theoretical models for PORs.

In [6] Castro M. and Liskov B. (2002) proposed an online services accessible on the Internet demands highly available systems that provide correct service without interruptions. Software bugs, operator mistakes, and malicious attacks are a major cause of service interruptions and they can cause arbitrary behavior, that is, Byzantine faults. It has a new replication algorithm, BFT, that can be used to build highly available systems that tolerate Byzantine faults.

In [7] Dodis Y., et al., (2009) proposed to allow the client to store a file F on an untrusted server, and later run an efficient audit protocol in which the server proves that it possesses the client's data. Constructions of PoR schemes attempt to minimize the client and server storage, the communication complexity of an audit, and even the number of file-blocks accessed by the server during the audit. In this work, it identifies several different variants of the problem (such as bounded-use vs. unbounded-use, knowledge-soundness vs. information-soundness), and giving nearly optimal PoR schemes for each of these variants. Constructions either improve (and generalize) the prior PoR constructions, or give the first known PoR schemes with the required properties. In particular,

- Formally prove the security of an (optimized) variant of the bounded-use scheme of Juels and Kaliski [JK07], without making any simplifying assumptions on the behavior of the

adversary.

- Build the first unbounded-use PoR scheme where the communication complexity is linear in the security parameter and which does not rely on Random Oracles, resolving an open question of Shacham and Waters [SW08].
- Build the first bounded-use scheme with information-theoretic security.
- The main insight of our work comes from a simple connection between PoR schemes and the notion of hardness amplification, extensively studied in complexity theory. In particular, improvements come from first abstracting a purely information-theoretic notion of PoR codes, and then building nearly optimal PoR codes using state-of-the-art tools from coding and complexity theory.

In [8] Erway C, et al. (2009) proposed as storage-outsourcing services and resource-sharing networks have become popular, the problem of efficiently proving the integrity of data stored at trusted servers has received increased attention. In the provable data possession (PDP) model, the client preprocesses the data and then sends it to an entrusted server for storage, while keeping a small amount of meta-data. The client later asks the server to prove that the stored data has not been tampered with or deleted (without downloading the actual data).

In [9] Juels A. and Burton J., Kaliski S. (2007) proposed POR scheme enables an archive or back-up service (provider) to produce a concise proof that a user (verifier) can retrieve a target file F, that is, that the archive retains and reliably transmits file data sufficient for the user to recover F in its entirety. A POR may be viewed as a kind of cryptographic proof of knowledge (POK), but one specially designed to handle a large file (or bit string) F. POR protocols here in which the ‘ communication costs, number of memory accesses for the provider, and storage requirements of the user (verifier) are small parameters essentially independent of the length of F.

In [10] Lillibridge M., et al. (2003) proposed a novel peer-to-peer backup technique that allows computers connected to the Internet to back up their data cooperatively: Each computer has a set of partner computers, which collectively hold its backup data. In return, it holds a part of each partner’s backup data. By adding redundancy and distributing the backup data across many partners, a highly-reliable backup can be obtained in spite of the low reliability of the average Internet machine.

In [11] Schwarz T. and Miller E.L. (2006) proposed the emerging use of the Internet for remote storage and backup has led to the problem of verifying that storage sites in a distributed system indeed store the data; this must often be done in the absence of knowledge of what the data should be. The scheme primarily utilizes one such algebraic property: taking a signature of parity

gives the same result as taking the parity of the signatures. It has three advantages over existing techniques. First, it uses only small messages for verification, an attractive property in a P2P setting where the storing peers often only have a small upstream pipe. Second, it allows verification of challenges across random data without the need for the challenger to compare against the original data. Third, it is highly resistant to coordinated attempts to undetectably modify data.

In [12] Shah M.A., et al. (2007) proposed a growing number of online service providers offer to store customers' photos, email, system backups, and other digital assets. Currently, customers cannot make informed decisions about the risk of losing data stored with any particular service provider, reducing their incentive to rely on these services. Here the third party auditing is important in creating an online service oriented economy, because it allows customers to evaluate risks, and it increases the efficiency of insurance based risk mitigation. It describes approaches and system hooks that support both internal and *external* auditing of online storage services, describe motivations for service providers and auditors to adopt these approaches, and list challenges that need to be resolved for such auditing to become a reality.

In [13] Shah M.A., et al. (2008) proposed a growing number of online services, such as Google, Yahoo!, and Amazon, are starting to charge users for their storage. Customers often use these services to store valuable data such as email, family photos and videos, and disk backups. Today, a customer must entirely trust such external services to maintain the integrity of hosted data and return it intact.

In [14] Shacham H. and Waters B. (2008) proposed a proof-of-retrievability system, a data storage center must prove to a verifier that he is actually storing all of a ˢalienfs data. The central challenge is to build systems that are both efficient and provably secure - that is, it should be possible to extract the client's data from any approver that passes a verification check. First scheme, built from BLS signatures and secure in the random oracle model, has the shortest query and response of any proof-of-retrievability with public verifiability. Next scheme, which ^builds elegantly on pseudorandom functions (PRFs) and is secure in the standard model, has the shortest response of any proof-of-retrievability scheme with private verifiability (but a longer query).

In [15] Wang C, et al. (2010) proposed the users have no physical possession of the possibly large size of outsourced data makes the data integrity protection in Cloud Computing a very challenging and potentially formidable task, especially for users with constrained computing resources and capabilities.

In [16] Bill Loeffler, et al. (2011) proposed infrastructure as service we need to drill into

specific charactereristics that a cloud platform provider must provide to be considered infrastructure as a service. This has been no easy task as nearly every cloud platform provider has recently promoted features and services designed to address the infrastructure as a service and cloud computing market. Fortunately, as the technology has evolved over time, a definition of cloud computing has emerged from the National Institute of Standards and Technology (NIST) that is composed of five essential characteristics, three service models, and four deployment models.

3. Implementation

3.1 General

To ensure the security and dependability for cloud data storage under the aforementioned adversary model, we aim to design efficient mechanisms for dynamic data verification and operation and achieve the following goals: (1) Storage correctness: to ensure users that their data are indeed stored appropriately and kept intact all the time in the cloud. (2) Fast localization of data error: to effectively locate the malfunctioning server when data corruption has been detected. (3) Dynamic data support: to maintain the same level of storage correctness assurance even if users modify, delete or append their data files in the cloud. (4) Dependability: to enhance data availability against Byzantine failures, malicious data modification and server colluding attacks, i.e. minimizing the effect brought by data errors or server failures. (5) Lightweight: to enable users to perform storage correctness checks with minimum overhead.

3.2 Problem Definition

Although outsourcing data into the cloud is economically attractive for the cost and complexity of long-term large-scale data storage, its lacking of offering strong assurance of data integrity and availability may impede its wide adoption by both enterprise and individual cloud users. In order to achieve the assurances of cloud data integrity and availability and enforce the quality of cloud storage service, efficient methods that enable on-demand data correctness verification on behalf of cloud users have to be designed. The verification of cloud storage correctness must be conducted without explicit knowledge of the whole data files . Meanwhile, cloud storage is not just a third party data warehouse.

3.3 methodologies

Methodologies is the process of analyzing the principles or procedure of a Secure and Dependable Storage Services in Cloud Computing.

- User Interface

- Third party auditing
- Identification of server
- Flexible distributed storage service
- Dynamic data manipulation

➢ **User Interface Design**

The User Interface design is done in this module. We use the Swing package available in Java to design the User Interface. Swing is a widget toolkit for Java. It is part of Sun Microsystems' Java Foundation Classes (JFC) — an API for providing a graphical user interface (GUI) for Java programs.

➢ **Third party auditing**

User can delegate the data auditing tasks to an optional trusted TPA of their respective choices. The storage verification task can be successfully delegated to third party auditing in a privacy-preserving manner. After login to the cloud service provider user can approach the Third party auditing. Third party auditing will be provide unique token to the each user. After getting the token, User should be provide proper token. Token should be validated each time in Third party cloud.

➢ **Identification of server**

In order to achieve assurance of data storage correctness and data error localization simultaneously, our scheme entirely relies on the pre-computed verification tokens. Stored data may store in some entrusted server .so we cloud service provider should concentrate on this issues. So cloud service provider must provide security for our data. In order to overcome this problem CSP must encrypt user data.

➢ **Flexible distributed storage service**

We propose in this paper flexible distributed storage integrity auditing mechanism, utilizing the homomorphic token and distributed erasure-coded data. This is used to data availability .After successful token validation by TPA next corresponding page will be displayed. In that user can upload the data.Data or file will be stored in corresponding cloud server. This is because data which is stored by user may stored in different storage space which is present in cloud server.

➢ **Dynamic data manipulation**

In this module we are are implementing Dynamic data Manipulation like block append, Insertion, deletion. This is employed to data updating. While storing the data in cloud server

there is a chance to store data in some other misbehaving server. The updated data will stored in corresponding server. Because user data may scattered in different storage server. So we have to analysis where our data stored . After analysis this process data will , down-loaded successfully.

4. Conclusion And Future Work

The importance of ensuring the remote data integrity has been highlighted by the following research works under different system and security models. These techniques, while can be useful to ensure the storage correctness without having users possessing local data, are all focusing on single server scenario. They may be useful for quality-of-service testing but does not guarantee the data availability in case of server failures. The deployment of Cloud Computing is powered by data centers running in a simultaneous, cooperated and distributed manner. It is more advantages for individual users to store their data redundantly across multiple physical servers so as to reduce the data integrity and availability threats. Thus, distributed protocols for storage correctness assurance will be of most importance in achieving robust and secure cloud storage systems.

In future users no need to spend time to encrypt their data. Instead], cloud service provider will provide security for our data. This is employed to reduce the computational cost.

References

1. Ateniese G., Bums R., Curtmola R., Herring J., Kissner L., Peterson Z. and Song D. (2007), 'Provable data possession at untrusted stores' in Proc. of CCS'07, Alexandria, VA, pp. 598-609.
2. Ateniese G., Pietro R.D., Mancini L.V. and Tsudik G. (2008), 'Scalable and efficient provable data possession' in Proc. of SecureComm'08, pp. 1-10.
3. Bellare M., Goldreich O. and Goldwasser S. (1994), 'Incremental cryptography: The case of hashing and signing' in Proc. of CRYPTO'94, Volume 839 of LNCS. Springer-Verlag, pp. 216- 233.
4. Bowers K.D., Juels A. and Oprea A. (2009), 'Hail: A high-availability and integrity layer for cloud storage' in Proc. of CCS'09, pp. 187-198.
5. Bowers K.D., Juels A. and Oprea A. (2009), 'Proofs of retrievability: Theory and implementation' in Proc. of ACM workshop on Cloud Computing security (CCSW'09), pp. 43-54. *
6. Castro M. and Liskov B. (2002), 'Practical byzantine fault tolerance and proactive recovery' ACM Transaction on Computer Systems, Vol. 20, No. 4, pp. 398^61.
7. Dodis Y., Vadhan S. and Wichs D. (2009), 'Proofs of retrievability via hardness amplification' in Proc. of the 6th Theory of Cryptography Conference (TCC'09), San Francisco, CA, USA.
8. Erway C, Kupcu A., Papamanthou C. and Tamassia R. (2009), 'Dynamic provable data possession' in Proc. of CCS'09, pp. 213-222.

9. Juels A. and Burton J., Kaliski S. (2007), 'Pors: Proofs of retrievability for large files' in Proc. of CCS'07, Alexandria, VA, pp. 584-597.

10. Lillibridge M., Elnikety S., Birrell A., Burrows M. and Isard M. (2003), 'A cooperative internet backup scheme' in Proc. of the 2003 USENIX Annual Technical Conference (General Track), pp. 29-41.

11. Schwarz T. and Miller E.L. (2006), 'Store, forget, and check: Using algebraic signatures to check remotely administered storage' in Proc. of ICDCS'06, pp. 12-12.

12. Shah M.A., Baker M., Mogul J.C. and Swaminathan R. (2007), 'Auditing to keep online storage services honest' in Proc. of HotOS'07. Berkeley, CA, USA: USENIX Association, pp. 1-6.

13. Shah M.A., Swaminathan R. and Baker M. (2008), 'Privacy-preserving audit and extraction of digital contents," Cryptology ePrint Archive, Report 2008/186, http://eprint.iacr.org/

14. Shacham H. and Waters B. (2008), 'Compact proofs of retrievability' in Proc. of Asiacrypt'08, Volume 5350 of LNCS, pp. 90-107.

15. Wang C, Wang Q., Ren K. and Lou W. (2010), 'Privacy-preserving public auditing for storage security in cloud computing' in Proc. of IEEE INFOCOM'10, San Diego, CA, USA.

16. Bill Loeffler October (2011). "Technet Magazine". http://technet.microsoft.com/en.us.

MHD BOUNDARY LAYER FLOW OF NANOFLUID PAST A INFINITE VERTICAL PLATE WITH CHEMICAL REACTION, HEAT SOURCE, RADIATION AND OHMIC DISSIPATION EFFECTS

S.Anuradha[1] and P.Priyadharshini[2]

Abstract

We have investigated a two dimensional MHD boundary layer flow on a vertical plate with effects of radiation, chemical reaction, viscous and ohmic dissipation effects and heat source. In this problem, the nanofluid model includes with Brownian and thermophoresis effects. A mathematical formulation has designed for momentum, temperature and nanofluid solid volume profiles. The coupled partial differential equations are solved using NDsolve in Mathematica. The results for the dimensionless velocity, temperature, and nanofluid solid volume profiles are discussed with the help of graphs. Various parameter values Prandtl Number, Nusselt number, skin friction coefficient are presented in tabular forms with thermophoresis parameter, magnetic parameter, Eckert number, Levis number, Chemical reaction parameter, Buoyancy-ratio parameter, heat generation/ absorption parameter.

Keywords

Nanofluid, Magentohydrodynamics (MHD), vertical plate, chemical reaction, heat source, Thermal Radiation.

I. Introduction

A Nanofluid is a fluid containing nanometer sized particles called as nano particles. These fluids are colloidal suspensions of nanoparticles in a base fluid. The nano particles used in nanofluids are typically made of metals, oxides, carbides or carbon nano tubes. Common base fluids include water, ethylene glycol and oil.Nanofluid is a two-phase mixture in which the solid phase consists of nano-seized particles. Nanofluid technology can help to develop better oils and lubricants Magneto Hydrodynamics (MHD) is the academic discipline concerned with the dynamics of electrically conducting fluids include magnetic field. These fluids include salt water, liquid metals and ionized

[1] *Prof & Head, Department of Mathematics, Hindusthan College of Arts & Science, Coimbatore. email:anu.prasanthi@gmail.com*

[2] *AP in Department of S&H, Sri Shakthi Institute of Engineering &Technology, Coimbatore. email:priyapsathish@gmail.com*

gases or plasmas. Nanofluid technology will help to develop better oils and lubricants. The use of nanofluids as coolants would allow for smaller size and better positioning of radiators.Nanofluids are used for cooling of microchips in computers and elsewhere.

The term nanofluid has been introduced by Choi[1].This novel fluid have been used potentially in numerous application in heat and mass transfer as well as micro electronics, fuel cells, Pharmaceutical sections. Sakisdis [2] was the first another to analyze the boundary layer flow on a continuous moving surface. Crane [3] found an exact solution of the boundary layer flow of the Newtonian fluid caused by the stretching of an elastic sheet moving in its own plane linearly. Buongiorno [4] was first who formulated the nanofluid model taking into account the effects of Brownian motion and thermophoresis. In his work he indicated that although there are some elements those affect nanofluid flow such as inertia, Brownian diffusion, thermophoresis, diffusiporesis, Magnus effect, fluid drainage and gravity only. Brownian diffusion and thermophoresis are important mechanisms in nanofluids. Wang [5] investigated the free convection flow on a vertical stretching surface.

Pop et al [6] obtained similarity solution by considering viscosity as an inverse function of temperature of the plate. There are several numerical studies on the modeling of natural convection heat transfer in naofluids. Gbadeyan et al [7] numerically studied natural convection flow of a nanofluid over a vertical plate with a uniform surface heat flux. Fang et al [8] used a second order a slip flow in their research. Choi and Eastman [9] discovered that the addition of less than 1% of nanoparticles into the base fluid doubles the heat conductivity of the fluid. Hamad et al [10] obtained the flow and mass transfer over a permeable sheet without fluid slip.Soundalgekar et al [11] studied the problem of flow of incompressible viscous fluid past a continuously moving semi-infinite plate by considering variable viscosity and variable temperature. Muthucumaraswamy [12] studied the effects of chemical reaction on vertical oscillating plate with variable temperature.Makinde [13] studied the effects of temperature dependent viscosity on free convective flow past a vertical porous plate in the presence of a magnetic field, thermal radiation and a first order homogeneous chemical reaction.Makinde and Mutuku [14] discovered the hydromagnetic thermal boundary layer of nanofluids over a convectly heated flat plate with viscous dissipation and ohmic heating effects. Geetha and Moorthy [15] studied hydromagnetic flow and heat transfer on a continuously moving surface with chemical reaction.Kuznetsov and Nield [16] obtained natural convective boundary layer flow of a nanofluid past a vertical plate.

Ganga *et al.* [17] investigated the effects of steady two dimensional radiative MHD boundary layer flow of viscous incompressible flow with internal heat generation/absorption over a vertical plate by using HAM method and compared the results by using fourth order RK-shooting method.

In this paper, we have extended Ganga *et al.*[17] work for two dimensional MHD boundary layer flow on a vertical plate with effects of radiation, chemical reaction, viscous and ohmic dissipation effects and heat source and the coupled partial differential equations are solved numerically by using NDsolve in Mathematica. The results for the dimensionless velocity, temperature, and nanofluid solid volume profiles are discussed with the help of graphs.

II. Mathematical Formulation

Consider a two dimensional steady magneto hydrodynamic boundary layer flow of a nanofluid which is electricity conducting (σ) and past a continuously moving surface with the uniform velocity U in the presence of magnetic field of strength B_0 is applied parallel to the y axis and chemical reaction with heat source is considered in the flow region it is assumed that the induced magnetic field, the external electric field are negligible due to polarization of charges. Let us consider x axis to be focused along the surface and y axis normal to the surface.

The governing equation of conservation of mass, momentum, energy and nano particle volume in the presence of magnetic field towards a continuously moving surface can be written in Cartesian coordinates x & y.

$$\frac{\partial u}{\partial x}+\frac{\partial v}{\partial y}=0 \tag{1}$$

$$\frac{\partial p}{\partial x}=\mu\left(u\frac{\partial u}{\partial x}+v\frac{\partial v}{\partial y}\right)-\sigma_e B_0^2 u+u[(1-C_\infty)\rho f_\infty \beta g(T-T_\infty)-\left(\rho_f-\rho f_\infty\right)g(C-C_\infty)$$

$$u\frac{\partial T}{\partial x}+v\frac{\partial T}{\partial y}=\frac{\partial}{\partial y}\left(\propto\frac{\partial T}{\partial y}\right)+\frac{u}{\rho c_\phi}\left(\frac{\partial u}{\partial y}\right)^2+\frac{\sigma_e B_0^2 u^2}{\rho c_\phi}+T\left\{D_B\left(\frac{\partial T}{\partial y}\frac{\partial C}{\partial y}\right)+\frac{D_T}{T_\infty}\left(\frac{\partial T}{\partial y}\right)^2\right\}+\frac{Q_0}{(\rho c)_f}(T-T_\infty)-\frac{1}{(\rho c)_f}\left(\frac{\partial q_r}{\partial y}\right) \tag{2}$$

(3)

$$u\frac{\partial C}{\partial x}+v\frac{\partial C}{\partial y}=D_B\frac{\partial^2 C}{\partial y^2}+\frac{D_T}{T_\infty}\frac{\partial^2 T}{\partial y^2}-K_r(C-C_\infty) \tag{4}$$

And the Boundary conditions are:

$$u=0, v=0, T=T_w(x), C=C_w(x)\ at\ y=0$$

$$u=v=0\ , T\to T_\infty\ , C\to C_\infty\ as\ y\to\infty \tag{5}$$

Where u and v are velocity components along x and y directions, α is a thermal diffusivity, Q_0 is a heat generation coefficient, ρ is the density of nanofluid, ρ_p is the nanoparticle density, ρ_c is specific heat of nanofluid at constant pressure, τ is the ratio of nanoparticle heat capacity, σ_e is the electrical conductivity, C_p is the specific heat and constant pressure, β is volumetric thermal expansion coefficient, μ is the thermal viscosity, D_B is the Brownian diffusion coefficient , D_T is the thermophoresis diffusion coefficient and K_r is the rate of chemical reaction.

The Radiative heat flux term by using The Rosseland approximation is given by

$$q = \frac{4\sigma^*}{3k_1^*}\frac{\partial T^{*^2}}{\partial y^*} \tag{6}$$

Where σ^* and $k_1^*$are the Stefan-Boltzmann constant and the mean absorption coefficient respectively. We assume that the temperature difference within the flow are sufficiently small such that T^{*^4} may be expressed as a linear function of the temperature. This is accomplished by expanding in a Taylor Series about T_∞^* and neglecting higher order terms.Thus,

$$T^{*4} \cong 4T_\infty^{*4} - 3T_\infty^{*4} \tag{7}$$

By using equation (6) and (7), into equation (3) is reduced to

$$u\frac{\partial T}{\partial x} + v\frac{\partial T}{\partial y} = \frac{\partial}{\partial y}\left(\propto \frac{\partial T}{\partial y}\right) + \frac{u}{\rho c_\phi}\left(\frac{\partial u}{\partial y}\right)^2 + \frac{\sigma_e B_0^2 u^2}{\rho c_\phi} + T\left\{D_B\left(\frac{\partial T}{\partial y}\frac{\partial C}{\partial y}\right) + \frac{D_T}{T_\infty}\left(\frac{\partial T}{\partial y}\right)^2\right\} + \frac{Q_0}{(\rho c)_f}(T - T_\infty) - \frac{1}{(\rho c)_f}\left(-\frac{16\sigma^* T_\infty^{*^3}}{3k_1^*}\right)\frac{\partial^2 T^*}{\partial y^2} \tag{8}$$

The equations (2), (4) and (9) can be transformed into the ordinary differential equation by using the following similarity transformations.

$$\left.\begin{aligned} \eta &= \frac{y}{x}(Ra_x)^{1/4}, \quad \Psi = \alpha(Ra_x)^{1/4} f(\eta) \\ \theta(\eta) &= \frac{T - T_\infty}{T_w - T_\infty}, \varphi(\eta) = \frac{C - C_\infty}{C_w - C_\infty} \end{aligned}\right\} \tag{9}$$

with the local Rayleigh number which is defined as

$$Ra_x = \frac{(1 - C_\infty)g\beta(T_w - T_\infty)}{v\alpha} \tag{10}$$

And the stream function $\Psi(x, y)$ is defined such that

$$u = \frac{\partial \Psi}{\partial y}, \qquad v = -\frac{\partial \Psi}{\partial x} \tag{11}$$

From the above transformations the non dimensional, non linear, coupled differential equations are obtained as:

$$f''' + \frac{1}{Pr}\left(3ff'' - 2f'^2 - 4M\sqrt{Pr}\, f'\right) + \theta - Nr\varphi = 0 \tag{12}$$

$$\left(1 + \frac{4N}{3}\right)\theta'' + \frac{3}{4}f\,\theta' + Nb\varphi'\theta' + Ecf''^2 + \frac{EcM}{\sqrt{Pr}}f'^2 + \lambda\sqrt{Pr}\,\theta = 0 \tag{13}$$

$$\varphi'' + \frac{3}{4} Le\, f\varphi' + \left(\frac{Nt}{Nb}\right)\theta'' - LeK\varphi = 0 \tag{14}$$

Where

$E_C = \frac{(1-C_\infty)g\beta x}{c}$ $(Eckert\ number)$; $Nt = \frac{(\rho C)_\rho D_T (T_w - T_\infty)}{(\rho C)_f \alpha T_\infty}$ $(Thermo\ phoresis\ parameter)$

$\lambda = \frac{Q_0 x^{1/2}}{(\rho c)_f \sqrt{(1-C_\infty)g\beta(T_w - T_\infty)}}$ $(Heat\ Source\ Parameter)$; $Le = \frac{\alpha}{D_B}$ $(Lewis\ number)$

$N = \frac{4\sigma^* {T_\infty}^3}{k\delta}$ $(Radiation\ parameter)$; $Nr = \frac{(\rho_p - \rho f_\infty)(C_w - C_\infty)}{(1-C_\infty)\rho f_\infty \beta(T_w - T_\infty)}$ $(Buoyancy\ ratio\ parameter)$

$Nb = \frac{(\rho C)_\rho D_B (C_w - C_\infty)}{(\rho C)_f \alpha}$ $(Brownian\ motion\ parameter)$; $P_r = \frac{v}{\alpha}$ $(Prandtl\ number)$

The corresponding Boundary conditions are

$$\left.\begin{aligned} f = \frac{4}{3} f_w, f' = 0, \theta = 1, \varphi = 1\ at\ \eta = 0 \\ f = 0, \theta = 0, \varphi = 0\ as\ \eta \to \infty \end{aligned}\right\} \tag{15}$$

The physical quantities of the local Nusselt number (Nu), and the local Sherwood number (Sh) are calculated by the following equations:

$$\begin{aligned} Nu(Ra_x)^{1/4} &= -\left(1 + \frac{4N}{3}\right)\theta'(0) \\ S_h(R_{e_x})^{-1/2} &= -\varphi'(0) \end{aligned} \tag{16}$$

III. Numerical Analysis

The set of non dimensional, non linear couple boundary layer equations (12) – (14) subject to boundary conditions (15) has been solved using NDsolve in Mathematica. The validity of the present computations has been confirmed via benchmarking with several earlier studies. The entire computation procedure is implemented using a program written and carried out using Mathematica computer language. From the process of computation the fluid velocity, the temperature, the concentration, the Skin friction coefficient, Nusselt number and Sherwood number are proportional to f'(η) , θ (η) , Φ (η) f''(η) , θ' (η) , Φ' (η).

IV. Results and Discussions

The heat and mass transfer problem associated with MHD flow of the nanofluids over a continuously moving surface has been studied. Table 1 indicates the values of skin friction, Nusselt Number and Sherwood Number for different values of the physical parameters.

Figure 1 shows dimensionless velocity profile for different values of suction/injection parameter (f_w) .It is observed that suction/injection parameter increases when the velocity decreases. Figure 2 displays dimensionless velocity distribution for different values of Magnetic parameter (M).It is noted that that Magnetic parameter increases when the velocity increases.

Figure 3 exhibits dimensionless velocity profile for different values of heat generation/absorption parameter (λ). It is observed that heat generation/absorption parameter increases when the velocity increases. Figure 4 displays dimensionless velocity distribution for different values of Eckert number (Ec). It is noted that that exponent parameter increases when the velocity increases. Figure 5 shows dimensionless velocity distribution for different values of Brownian motion parameter (Nb). It is observed that that Brownian motion parameter increases when the velocity decreases.

Figure 6 exhibits dimensionless velocity profile for different values of Buoyancy ratio parameter (Nr). It is observed that Buoyancy ratio parameter increases when the velocity increases. Figure 7 displays dimensionless velocity distribution for different values of thermophoresis parameter (Nt). It is noted that that thermophoresis parameter increases when the velocity increases.

Figure 8 shows dimensionless temperature profiles for different values of Magnetic parameter (M). It is observed that Magnetic parameter increases when the temperature increases. Figure 9 shows dimensionless temperature profiles for different values of Eckert number (Ec). It is observed that Eckert number increases when the temperature decreases.

Figure 10 shows dimensionless temperature distribution for different values of Brownian motion parameter (Nb). It is observed that that Brownian motion parameter increases when the temperature decreases. Figure 11 displays dimensionless temperature distribution for different values of thermo phoresis parameter (Nt).It is noted that that thermophoresis parameter increases when the temperature increases.

Figure 12 exhibits dimensionless temperature profile for different values of heat generation/absorption parameter (λ). It is observed that heat generation/absorption parameter increases when the temperature increases. Figure 13 displays dimensionless concentration distribution for different values of Magnetic parameter (M).It is noted that that Magnetic parameter increases when the concentration increases.

Figure 14 displays dimensionless concentration distribution for different values of Eckert number (Ec).It is noted that that exponent parameter increases when the concentration decreases. Figure 15 exhibits dimensionless concentration profile for different values of Buoyancy ratio parameter (Nr). It is observed that Buoyancy ratio parameter increases when the concentration decreases.

Figure 16 exhibits dimensionless concentration profile for different values of heat generation/absorption parameter (λ). It is observed that heat generation/absorption parameter increases when the concentration decreases.

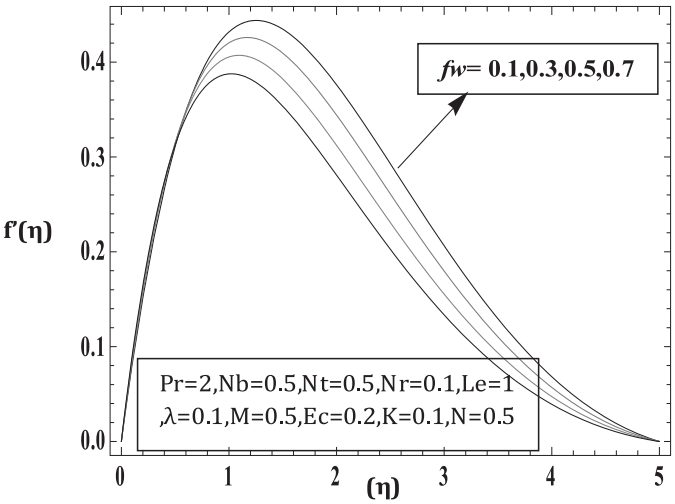

Fig.1:Effects of suction/injection parameter (*fw*) on velocity Profiles

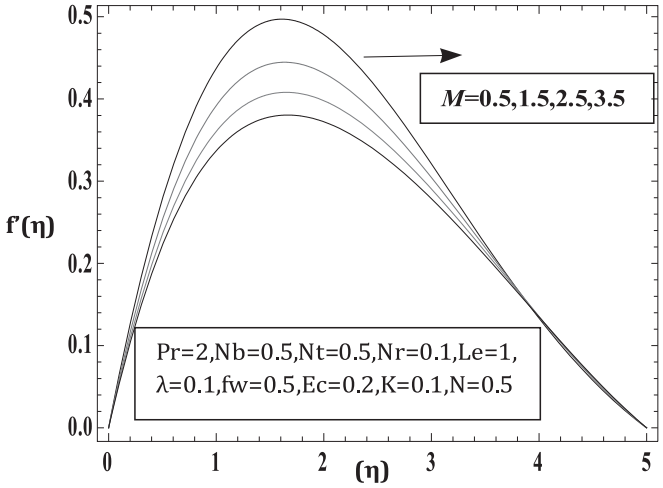

Fig.2: Effects of magnetic parameter (*M*) on velocity Profiles

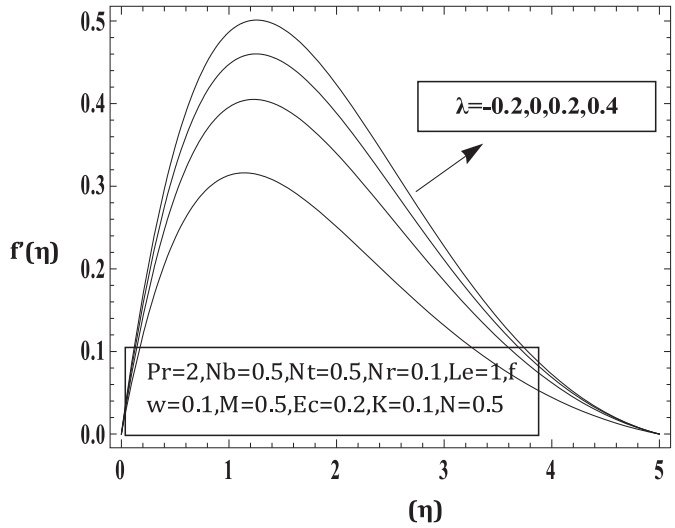

Fig.3: Effects of heat generation/absorption parameter (*λ*) on velocity Profiles

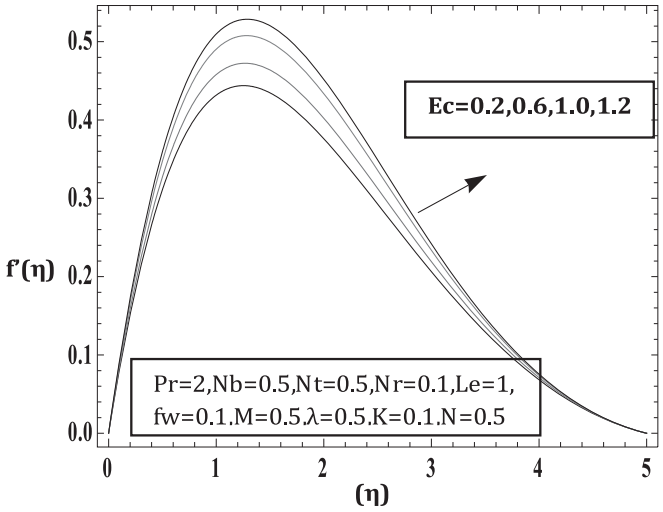

Fig.4: Effects of Eckert number (*Ec*) on velocity Profiles

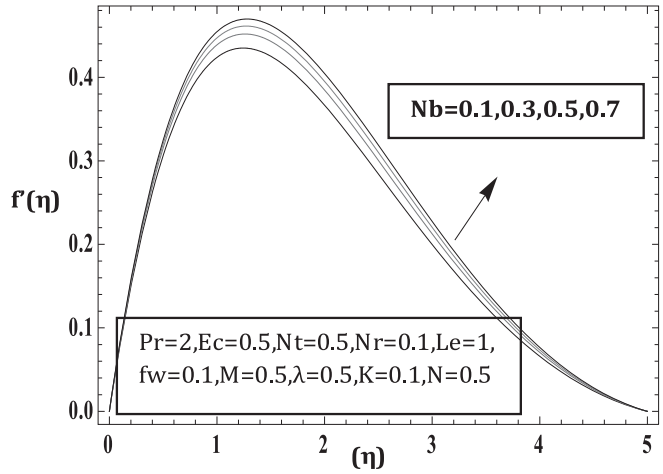

Fig.5: Effects of Brownian motion parameter (*Nb*) on velocity Profiles

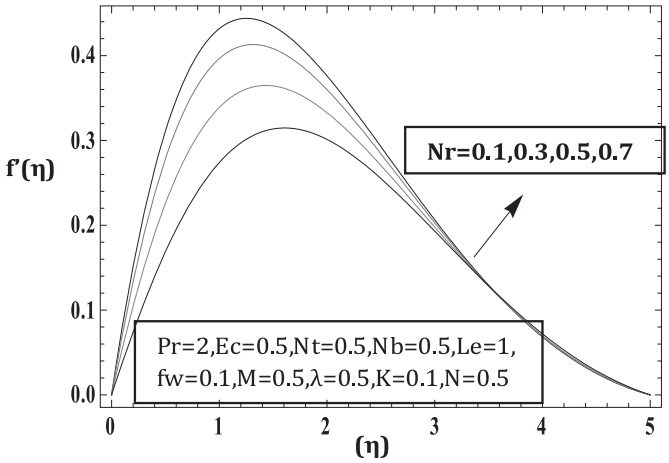

Fig.6: Effects of Buoyancy motion parameter (*Nr*) on velocity Profiles

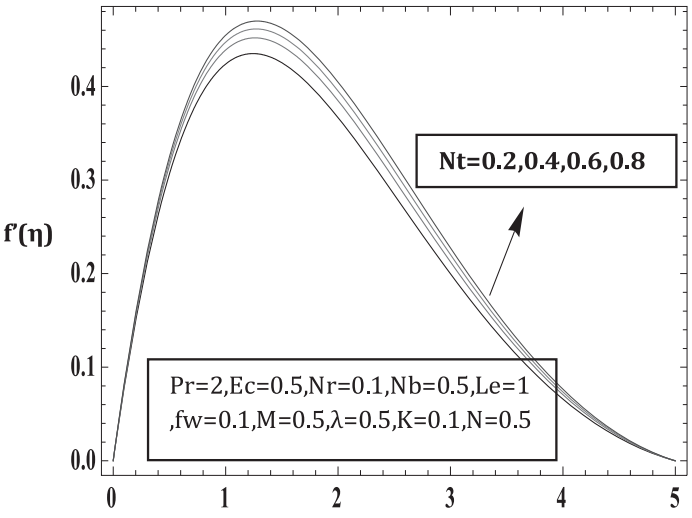

Fig.7: Effects of Thermo phoresisparameter (*Nt*) on velocity Profiles

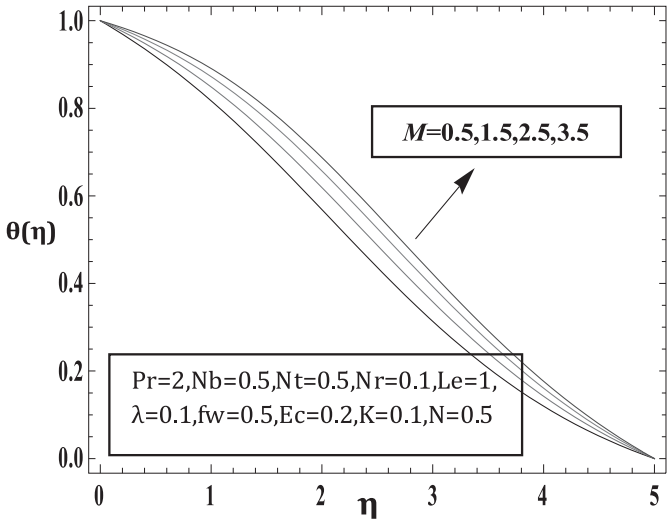

Fig.8: Effects of magnetic parameter (*M*) on temperature Profiles

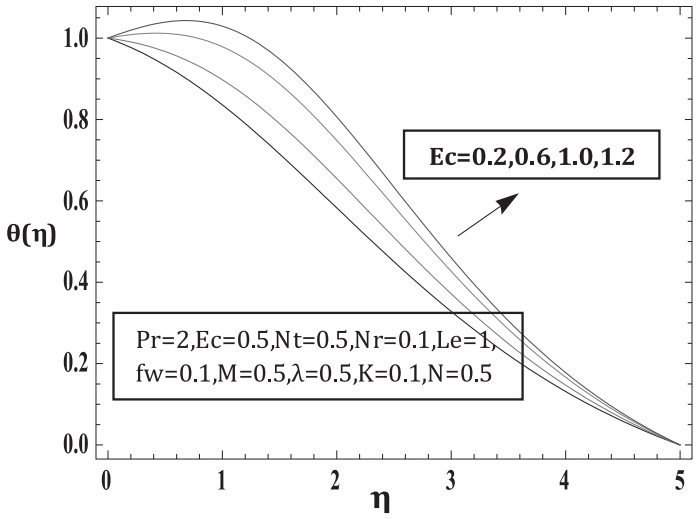

Fig.9: Effects of Eckert number (*Ec*) on temperature Profiles

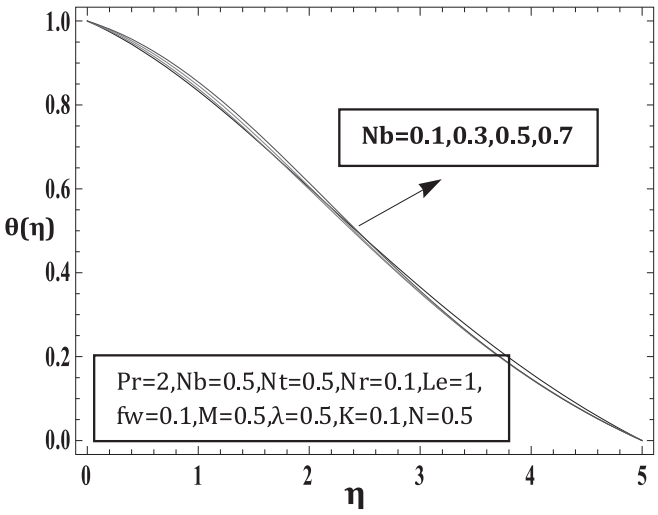

Fig.10: Effects of Brownian motion parameter (*Nb*) on temperature Profiles

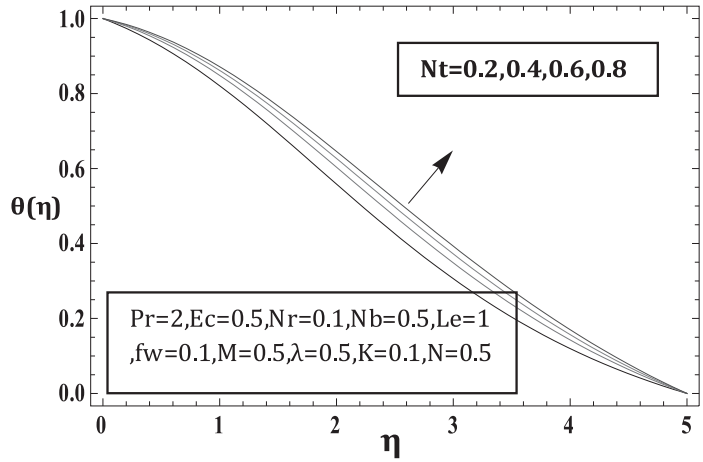

Fig.11: Effects of Thermo phoresis parameter (*Nt*) on temperature Profiles

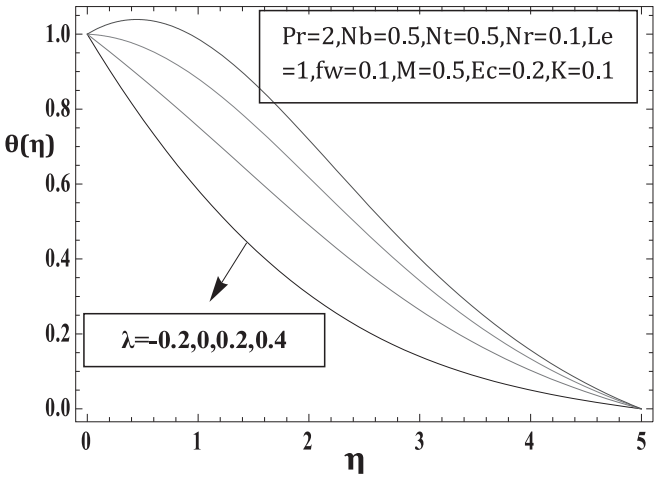

Fig.12: Effects of heat generation/absorption parameter (λ) on temperature Profiles

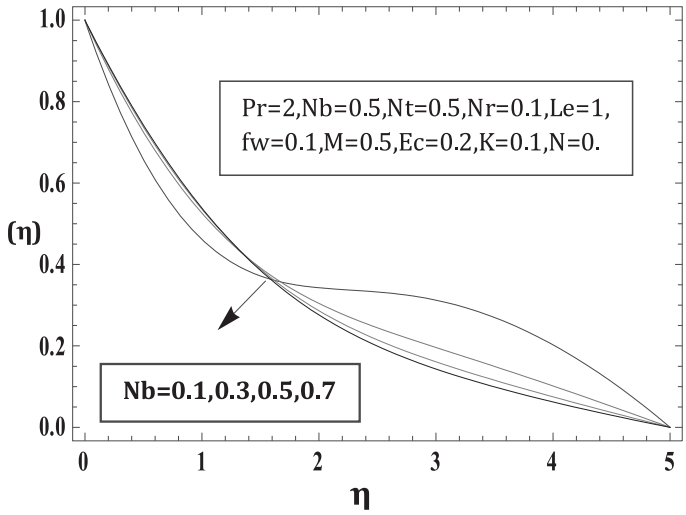

Fig.13: Effects of Brownian motion parameter (*Nb*) on concentration Profiles

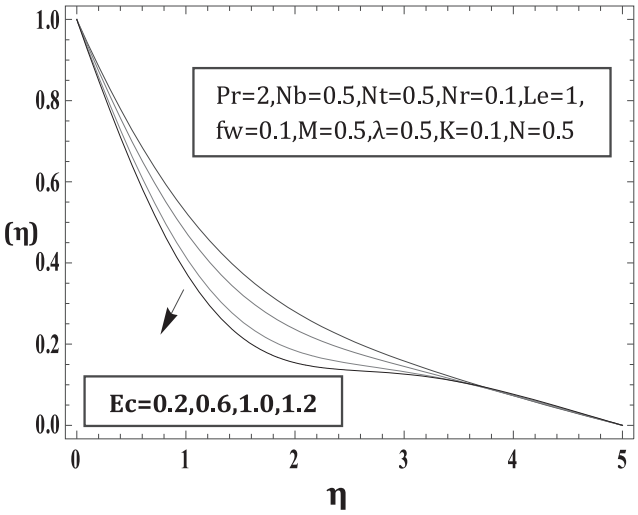

Fig.14: Effects of Eckert number (*Ec*) on concentration Profiles

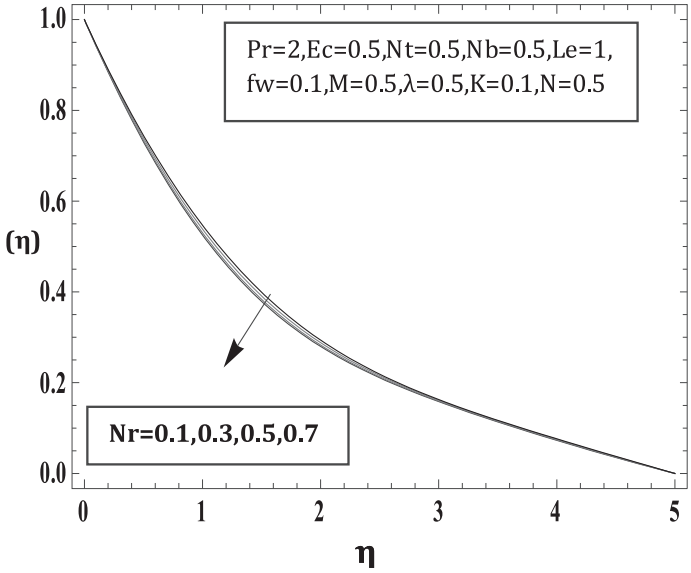

Fig.15: Effects of Buoyancy motion parameter (*Nr*) on concentration Profiles

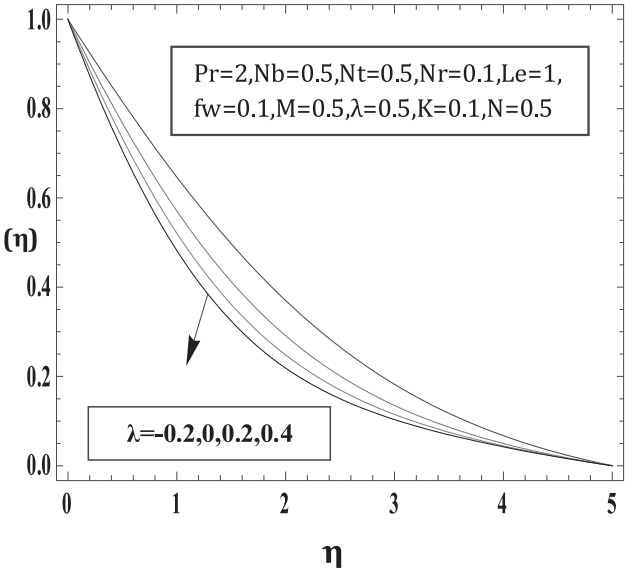

Fig.16: Effects of heat generation/absorption parameter (*λ*) on concentration Profiles

Table 1: The values of skin friction, Nusselt Number and Sherwood Number for different values of the physical parameters

fw	Pr	N	Nb	Nt	Le	λ	M	K	Nr	Ec	f'' (0)	θ'(0)	φ'(0)
0.1	2	0.5	0.1	0.5	1	0.5	0.5	0.1	0.5	0.3	0.666024	-0.003949	-1.33474
0.1	2	0.5	0.3	0.5	1	0.5	0.5	0.1	0.5	0.3	0.643358	-0.0534313	-0.846068
0.1	2	0.5	0.5	0.5	1	0.5	0.5	0.1	0.5	0.3	0.6403	-0.0762375	-0.720691
0.1	2	0.5	0.7	0.5	1	0.5	0.5	0.1	0.5	0.3	0.641006	-0.090764	-0.662629
0.1	2	0.5	0.5	0.1	1	0.5	0.5	0.1	0.5	0.3	0.846567	-0.116628	-0.545317
0.1	2	0.5	0.5	0.3	1	0.5	0.5	0.1	0.5	0.3	0.866251	-0.0877166	-0.671335
0.1	2	0.5	0.5	0.5	1	0.5	0.5	0.1	0.5	0.3	0.877226	-0.0746054	-0.772506
0.1	2	0.5	0.5	0.7	1	0.5	0.5	0.1	0.5	0.3	0.8885	-0.064918	-0.880886

V. Conclusion

In this study ,a mathematical model for a two dimensional MHD boundary layer flow on a vertical plate has been designed considering various physical parameters such as effects of radiation, chemical reaction, viscous and ohmic dissipation effects and heat source. The validity of the present computations has been confirmed via benchmarking based on several earlier studies. In our paper, the entire computation procedure is implemented using a program written in Mathematica software.

- The increase in magnetic parameter is to increase both velocity and temperature profiles and decrease in concentration profiles.
- The increasing values of Eckert number accelerate both the velocity and temperature of nanofluid.
- The increase in exponent parameter is to increase in temperature and decrease in concentration profiles.
- The increase of chemical reaction parameter is to increases in velocity and temperature profiles.
- The heat transfer coefficient of nanofluid increase with the increases of velocity and temperature profiles.
- The velocity and temperature profiles increase in the case of heat generation and decrease in the heat absorption case.

- Brownian motion and thermophoresis parameters increase both the velocity and temperature profiles and decrease the concentration profile.

References

1. **Choi SUS**. Enhancing thermal conducting of fluids with nanoparticles , development and applications of non-Newtonian flows.D.A. Singer and H.P.Wang, eds., ASMEMD-vol.231 and FED- vol.231 and FED-vol. 66, USDOE, Washington, DC (United States). 1995; 231;99-105.
2. **Sakiadis B.C**.Boundary layer behavior on a continuous solid surface.AICHE.J,vol.7.1961;7;221-225.
3. **Crane L.J**. Flow past a stretching plate .ZAMP, 1970;21;645-647.
4. **Buongiorno.J**. Convective transport in nanofluids, ASME Journal of Heat Transfer, 2006;18;240-250.
5. **Wang CY**. Free convective on a vertical stretching surface.Journal of Applied mathematics and Mechanics ,ZAMM, vol.69.1989;69;418-420.
6. **Pop I , Gorla RSR, Rashidi M**.The effect of variable viscosity on flow and heat transfer to a continuously moving flat plate.IntEng Sci.1992;30:1-6.
7. **Gbadeyan JA, Olanrewaju**, MA. Boundary layer flow of a nanofluids over a moving surface in a flowing fluid in the presence of magnetic field and thermal radiation AJBAS,2011;9:1323-1334.

Registered with Registrar of News Papers in India vide Registration No. TNBIL/2009/29041

ISSN 2277-7628